

**Deanship of Graduate Studies
Al-Quds University**



**Effect of the Surface Charge
Discretization (Mobile Charge) on Electric Double
Layer**

Mirfit Mahmoud Amleh

M.Sc Thesis

Jerusalem-Palestine

1431/2010

**Effect of the surface charge
discretization (mobile charge) on electric double layer**

**Prepared by:
Mirfit Mahmoud Amleh**

**B.Sc. Pharmacy King Saud University
Saudi Arabia**

Supervisor: Dr.Khawla Qamhieh

**A Thesis Submitted in Partial fulfillment of
requirement for the degree of Master of Applied
Industrial Technology, Al-Quds University**

1431/2010

Al-Quds University
Deanship of Graduate Studies
Applied and Industrial Technology Program



Thesis approval

Effect of the Surface Charge
Discretization (Mobile Charge) On Electric Double layer

Prepared by: Mirfit Mahmoud Amleh
Registration No: 20714132

Supervisor: Dr. Khawla Qamhieh

Master thesis submitted and accepted, date 28 / 6 /2010
The name and signature of examining committee member are as follows

1- Head of Committee: Dr.	Signature.....
2- Internal Examiner: Dr	Signature.....
3- External Examine: Dr	Signature.....

Jerusalem-Palestine

1431/2010

Dedication

I would like to dedicate this work to my mother, mother-in-law, my husband Fared Amleh and my children Sajeda, Noor, Kamelia, AbdAlnam, Mahmoud and Muhammad and my brother-in-law Ishaq Amleh and my brothers and sisters for their encouragement and stimulation throughout the duration of my writing up. ..Thanks all...

Mirfit Amleh

Declaration

I certify that this thesis submitted for the degree of Master is my own research, except where otherwise acknowledged, and that this thesis (or any part of the same) has not been submitted for higher degree to any other university or institution.

Signed: Mirfit Amleh

Date: 28-6-2010

Acknowledgment

Initially, I would especially like to thank my supervisor, Dr. Khawla Qamhieh who gave me an opportunity to do this work in which I am really interested, and make this thesis possible. Thanks for her guidance, suggestions, and valuable help during the course of higher studies program of applied industrial technology.

I owe thanks to a number of individuals in the department of Chemistry at the Al-QUDS University– Abu Deis both in general and with regard to my thesis.

I do not forget to thank my colleagues for their encouragement.

I thank my brother-in-law Ishaq for all his guidance, support, and stimulation. And I also thank my sister Ketahm.

Very special thanks are also due to my mother and mother-in-law for praying to demand luck and success for me.

Great many thanks I would like to give to my devoted husband fared. It has been his love and support (along with my children) that has provided me the incentive to complete my thesis. I sincerely cannot help expressing how I should credit this thesis to his support. I am extremely fortunate to have him in my life.

I am also very grateful to my children Sajeda, Noor, Kamelia, Abd Alnam, Mahmoud and Muhammad for their support, encouragement, stimulation and valuable help. They gave me confidence from the beginning and thus gave me the ability to continue studying and working hard. Thanks my love.

I am also greatly indebted to all my friends and family, who have supported me in all possible ways as needed. Above all, I thank God for making all this possible.

Abstract

The structure of the electric double layer (EDL) in contact with discrete and continuously charged sphere macroion surfaces is studied within the framework of the primitive model through Monte Carlo simulations.

Mobile charge discretization models (point charges localized on the macroion surface and finite-sized charges protruding into the solution) are considered together with the case of uniform charge distribution (central). The distribution of counterions near a macroion is determined using a spherical cell. The effect of discreteness is analyzed in terms of radial distribution functions, charge density profiles, and potential profiles. The effect of discretization, radius of the counterions and the presence of salt on the potential of EDL and accumulated charges are also studied.

It is established that with protruding charges the counterions are less accumulated near the macroion because the excluded volume effect dominating over the increased correlation ability. But with point charges distributions, counterions become more strongly accumulated to the macroion and the effect increases with counterion valence. At low salt concentration, the macroion accumulated charge is reduced due to multivalent counterion adsorption. At high salt concentrations, the macroions become overcharged so that their apparent charge has the opposite sign to the stoichiometric one. The character of charge distribution affects the EDL structure near the macroion, whereas its effect is much weaker at larger distances.

Table of Contents

Chapter one	
1. Introduction	2
1.1 Colloids	4
1.2 Charge inversion (phenomena of over charging)	4
1.3 Electric double layers	5
1.4 Models of the electrical double-layer	8
1.4.1 Helmholtz model	8
1.4.2 Gouy- Chapman model	9
1.4.3 Stern-Graham model	10
1.5 DLVO theory	11
1.6 Computer simulations	12
1.7 Statement of the problem	13
Chapter two	
2. Model and method	15
2.1 Method	15
2.2 Monte Carlo Simulation	15
2.2.1 Estimation of (π)	16
2.2.2 Metropolis algorithm	17
2.3 Model	17
Chapter three	
3 Result and discussions	21
3.1 Effect of valence and discretization.	21
3.2 Effect of adding salt.	41
3.3 Effect of the size of counterions.	53
Chapter four	
Conclusions	58
References	60

List of Tables

Table number	Table name	Page
Table 2.1	Name of the ensemble used in simulation.	15
Table 3.1	Values of the maximum accumulation of counterions g_{mi} in the vicinity of macroion for all charges distributions at counterion valence $Z_i = 1, 2$ and 3 .	25
Table 3.2	Ratio of counterions at $r = 25 \text{ \AA}$ for all charge distributions model for different counterions valences.	28
Table 3.3	Maximum local charge density ($\rho(r)$ in C/cm^3) accumulation of counterions in the vicinity of macroion for all charges distributions at different counterion valence.	32
Table 3.4	Values of Z_{eff} for the system with central charge distribution and discrete charge distribution at counterion valence (a) $Z_i = 1$, (b) $Z_i = 2$ and $Z_i = 3$ at $r = 25 \text{ \AA}$	35
Table 3.5	Potential for central charge distribution model and discrete charge distribution at counterion valence (a) $Z_i = 1$, (b) $Z_i = 2$ and $Z_i = 3$ at the surface of macroion (Ψ_0 <u>Surface potential</u>) $r = 22 \text{ \AA}$ and (Ψ_d <u>diffused potential</u>) at $r = 30 \text{ \AA}$	38
Table 3.6	Maximum counterions-counterions radial distributions for all charges distributions models at counterion valence $Z_i = 1, 2$ and 3 .	40
Table 3.7	Maximum counterions-counterions rdfs for the system of central charges distributions at counterion valence $Z_i = 1$ at $\beta = 0, 0.15$, and 0.45 .	45
Table 3.8	Maximum counterions-counterions rdfs for mobile protruding charges distributions model at counterion valence $Z_i = 1$ at $\beta = 0, 0.15$, and 0.45 .	46
Table 3.9	Maximum counterions-counterions rdfs for mobile surface charges distributions model at counterion valence $Z_i = 1, 2$ and 3 at $\beta = 0, 0.15$, and 0.45 .	47
Table 3.10	Effective charge for the system with central and discrete charge distributions at $\beta = 0, 0.75, 2.5, 6.25$.	49
Table 3.11	Electrostatic potential for the system with central and discrete charge distributions at counterion valence of $Z_i = 1$ at different concentrations of salt.	52
Table 3.12	Effective charge for the system with central charge distribution at counterion radius $= 1, 2$ and 3 \AA for $Z_i = +1$ at 25 \AA	54
Table 3.13	Potential for central charge distribution model and discrete charge distribution at counterion radius $1 \text{ \AA}, 2 \text{ \AA}$, and 3 \AA .	56

List of Figures

Figure number	Figure name	Page
Figure 1.1	Schematic representation of the positions of the Stern plane and the Zeta potential in the electric double layer.	6
Figure 1.2	The distribution of positive and negative ions around the charged macroion.	7
Figure 1.3	Schematic representation of the Helmholtz model of the electrical double-layer: (a) distribution of counterions in the vicinity of the charged surface; (b) variation of electrical potential with distance from the surface.	8
Figure 1.4	Schematic representation of the Gouy-Chapman model of the electrical double-layer: (a) distribution of counterions in the vicinity of the charged surface; (b) variation of electrical potential with distance from the surface.	9
Figure 1.5	Schematic representation of the Stern-Graham model of the electrical double-layer: (a) distribution of counterions in the vicinity of the charged surface; (b) variation of electrical potential with distance from the surface.	10
Figure 1.6	DLVO-type interaction (continuous line) obtained as the sum of the electrostatic repulsion and van der Waals attraction.	11
Figure 1.7	The connection between experiment, theory, and computer simulation.	13
Figure 2.1	Estimation of π	16
Figure 2.2	Metropolis algorithm is used to reject or accept a move.	17
Figure 2.3	Schematic illustration of the macroion charge distributions: (a) a central charge with R_M denoting the macroion radius, (b) point charges on the macroion surface, and (c) protruding charges with hard-sphere radius R_S . The r_s denotes the radial location of the macroion charge.	18
Figure 3.1	Macroion-counterion radial distribution functions at counterion valences (a) $Z_i = 1$, (b) $Z_i = 2$, (c) $Z_i = 3$ for central charge (c) distribution ----- (dashed curve), mobile point (ms)..... (dot curve) and mobile protruding (mp) Charge distribution_____.	22
Figure 3.2	Snapshots of systems containing one macroion (red sphere), monovalent counterions (blue sphere), protruding charges (Green sphere) at $Z_i = 1$ in case of (a) central charge distributions, (b) mobile point charge distributions and (c) mobile protruding charge distributions, all particles are enclosed in spherical cell.	23

Figure number	Figure name	Page
Figure 3.3	Snapshots of systems containing one macroion (red sphere), monovalent counterions (blue dots) at different valences of counterions (a) $Z_i = 1$ (b) $Z_i = 2$ (c) $Z_i = 3$ from central charge distributions.	24
Figure 3.4	Normalized counterion running coordination number $P(r)$ at counterion valences $Z_i = 1, 2, 3$ for central charge distribution (c) ----- (dashed curve), mobile point (ms)..... (dote curve) and mobile protruding (mp) - _____ charge distributions.	27
Figure 3.5	Relative normalized running coordination number at counterion valences (a) $Z_i=1$, (b) $Z_i=2$, and(c) $Z_i=3$ for the mobile surface and mobile protruding charge distributions as obtained from the spherical cell. $\Delta P(r) = P(r) - P_{\text{central charge}}(r)$.	29
Figure 3.6	local charge density at $Z_i = 1, 2, 3$ for the system with discrete and central charge distributions	31
Figure 3.7	Accumulated charge at $Z_i = 1, 2, 3$ for the system with central and discrete charge distributions	33
Figure 3.8	Accumulated charge for the system with (a) central (b) mobile surface (c) mobile protruding charge distribution models at different valence of counterion	34
Figure 3.9	The potential at counterion valence (a) $Z_i=1$, (b) $Z_i = 2$ and $Z_i = 3$ for central charge distribution model and discrete charge distribution.	36
Figure 3.10	Electrostatic potential for the systems with central and discrete charge distribution models at counterion valence $Z_i=1, 2, 3$ (a)central, (b)ms (c) mp	37
Figure 3.11	Counterion- counterion radial distribution functions for the systems at counterion valences $Z_i=1, 2, 3$ for (a) mobile surface, (b) uniform and (c) mobile protruding charge distributions	39
Figure 3.12	(a) Macroion-trivalent counterion (cation) and (b) macroion-monovalent counterion rdfs at the indicated amount of simple 1:3 electrolyte expressed as the trivalent counterion -to-macroion charge ratio β at $Z_i=1$ for the system with central charge distributions.	42
Figure 3.13	Macroion-coion radial distribution functions at indicated amount of simple 1:3 electrolyte expressed as the trivalent counterion -to-macroion charge ratio β at uniform and discrete Charge distributions	43

Figure number	Figure name	Page
Figure 3.14	Snapshots of systems containing one macroion (red sphere) , monovalent counterions (blue sphere) , trivalent counterions (White sphere) , coions (yellow sphere) , surface charge (Green sphere) at $Z_i=1$ in case of mobile protruding charge distributions at different amounts of the simple salt 1:3 electrolyte expressed as the trivalent counterions to macroion charge ratio (a) $\beta =0$, (b) $\beta=0.75$,and (c) $\beta=6.25$ all particles are enclosed in spherical cell.	44
Figure3.15	Shows the counterion-counterion radial distribution functions at counterions valence $Z_i =1$ from central charge distribution in the presence of salt at different concentrations, after the addition of 1:3 salt The value of the maximum of counterion-counterion radial distribution (g_{ii}) is decreased by increasing β .	45
Figure3.16	Shows the counterion-counterion radial distribution functions at counterions valence $Z_i =1$ from mobile protruding charge distribution in the presence of salt at different concentrations, after the addition of 1:3 salt The value of the maximum of counterion-counterion radial distribution (g_{ii}) is decreased by increasing β .	46
Figure3.17	Shows the counterion-counterion radial distribution functions at counterions valence $=1$ from surface charge distribution in the presence of salt at different concentrations, after the addition of 1:3 salt the value of the maximum of counterion-counterion radial distribution (g_{ii}) is decreased by increasing the value of β	47
Figure 3.18	Accumulated charge for (a) central and (b) mobile surface (c) mobile protruding charge distribution at different values of β	48
Figure 3.19	The potential for the system of central and discrete charge distributions at counterion valence $Z_i=1$ at $\beta=0$,and 0.75	50
Figure 3.20	Electrostatic potential for the system with central and discrete charge distributions at counterion valence of $Z_i=1$ at different concentrations of salt	51
Figure 3.21	Local charge density at $Z_i=1, 2, 3$ for the system with discrete and central charge distributions at different radii of counterions.	53
Figure 3.22	Accumulated charge for central charge distribution at different radii of counterion.	54
Figure 3.23	The electrostatic potential for the system with (a)uniform(central) (b) mobile surface (ms) and (c) mobile protruding (mp) charge distributions at different counterions radii (1,2and 3 Å)	55

Abbreviations

c	Central (uni form) surface charge distribution.
DLVO theory	Derjaguin Landau-Verwey-Overbeek theory.
DNA	Deoxyribonucleic acid.
ϵ_0	The permittivity of vacuum = $8.854 * 10^{-12}$ c/v.m.
ϵ_r	The relative permittivity= 78.4 at room
temperature	25C°
σ_M	Macroion surface charge density.
e	The elementary charge= $1.6 * 10^{-19}$ Coulomb.
EDL	Electric double layer .
IEP	Isoelectric Point.
MC	Monte Carlo .
mp	Mobile protruding charge distribution.
ms	Mobile surface charge distribution.
NVE	Constant number of particles, volume and energy.
NVT	Constant number of particles, volume and temperature.
NPT	Constant number of particles, pressure and temperature.
PB	Poisson-Boltzmann .
P(r)	Normalized counterions running coordination.
$\Delta P(r)$	Relative normalized running coordination number.
rcn	Running coordination number.
rdfs	Radial distribution functions.
R_M	Macroion radius.
R_S	Radius of charged site.
R_i	Counterions radius.
R_{ca}	Cations radius.
R_a	Anions radius.
R_{sph}	Spherical cell radius.
P_i	Counterion number density.
ρ_M	Macroion number density.
Φ_M	Macroion volume fraction.
T	The temperature =298 K in Kelvin.
U	Total potential.
U_{hs}	Hard-sphere repulsion.
U_{elec}	Coulomb interaction.
U_{ext}	External potential.
Z_M	Macroion charge.
Z_S	Charge of charged site .
Z_i	Counterions charge.
Z_{ca}	Cations charge.
Z_a	Anions charge.

Definitions

Colloids	Are defined as very small, finely divided solids (particles that do not dissolve) that remain dispersed in a liquid for a long time due to their small size and electrical charge.
Counterions	The small ions that have an opposite charge to the macroions.
Co-ions	The small ions that have a charge of the same sign of the macroions.
EDL	It is the layer caused by the accumulation of counterions and co ions in the vicinity of macroions.
Macroions	Stand for ions that are larger in radius and charge than other ions in the solution.
Monte Carlo simulations	It is stochastic technique (meaning it is based on the use of random numbers and probability statistics to investigate problems.
Primitive model	Model used to investigate intercolloidal structure of colloidal solutions. In this model, the charged colloids (referred to as macroions) and the small ions are both represented as hard spheres whereas the solvent is treated as a dielectric medium.

Chapter One

Chapter One

1. Introduction

Macroions stand for ions that are larger in radius and charge than counterions and coions their stability is governed by electrostatic interactions. Examples of macroions are proteins, nucleic acids, nanoparticles, asymmetric electrolytes, micellar solutions, microemulsions, and charged colloidal suspensions. They are of great importance in natural sciences, in technology and for production of pharmaceuticals, textile and food.

Charged colloidal suspensions (of the size 10–1000 nm) are a subject of intense experimental and theoretical work because of their direct application in industrial or biological processes. Examples of colloidal suspensions are proteins, microemulsions formed by water, oil, and charged surfactants, silica particles, latex particles, and micelles formed by charged surfactants. The electrostatic interactions involved in such systems have a fundamental role in determining their physico-chemical properties (Roj 2009)¹ (Shaw 1992)².

Theoretical description of these electrostatic interactions between a pair of charged particles in charged colloidal suspensions started more than ninety years ago with the Debye-Hückel theory (Debye and Huckel 1923)³. This is based on that the ions of completely dissociated electrolytes are assumed to be charged hard spheres and the solvent is treated as a dielectric continuum, which is in closest agreement with the Monte Carlo simulations.

Debye-Hückel theory realized that since the mean force inside the electrolyte is zero it is the correlations in positions of oppositely charged ions that produce the main contribution to the free energy. Its simplicity and linear structure allow it to avoid the internal inconsistencies that are often present in the more complicated non-linear theories of electrolytes. But the Debye-Hückel theory cannot account for non-linear configurations, such as the formation of dipoles. Then the scientist Bjerrum proposed that the missing non-linearities can be reintroduced into the Debye-Hückel theory through the assumption of chemical equilibrium between monopoles and multipoles. (Bjerrum, et.al. 1926)⁴

Further development of Debye-Huckel theory is the Poisson-Boltzmann (PB) equation, a mean-field theory that neglects ion-ion correlations, and treats the free ions (counterions and added salt) as point-charges. It states that the average solvent-mediated electrostatic potential between two macroions of similar charge is always repulsive but it cannot explain the phenomenon of overcharge.

At 1940s Derjaguin Landau-Verwey-Overbeek (DLVO) (Deryaguin and landau 1941)⁵, (Verwey and Overbeek 1948)⁶ theory gives an approximated analytical solution of Poisson-Boltzmann equation. Both Poisson-Boltzmann equation and DLVO theory provide a semi-quantitative description of the solvent-mediated potential between charged colloidal particles.

The mean-field description was contradicted by many researchers; they argued that because of the intervention of counterions, there could exist an electrostatic attraction

between like-charged particles at certain solution conditions. Kirkwood and Schumaker developed an analytical expression for the attractive force and demonstrated that the fluctuations in the net charges of macroions result in an attractive potential. (Ravindran and Wu 2005)⁷

In the late 1960s, Oosawa demonstrated that the correlated fluctuations of the small ion distributions around two macroions could lead to an electrostatic attraction (Ravindran and Wu 2005)⁷

After that Sogami and Ise proposed a variation of the DLVO theory. They predict a ubiquitous long-range attraction between like charges (Sogami and Ise, 1984)⁸ that is too weak and occurs at macroions separations that are too large. But Kjellander et al (Kjellander et.al. 1990)⁹ indicated that the electrical double layer interaction can be attractive at short surface separations if divalent counterions are present.

The additional contradictions from DLVO theory was the existence of an attraction of electrostatic nature between two like-charged planar surfaces originating from ion-ion correlations which has been demonstrated via simulation techniques (Guldbrand et.al. 1984)¹⁰, and liquid-state theories (Marcelja and Kjellander 1984)¹¹. Also attraction between like-charged macroions of the same origin was later confirmed by several simulation studies (Belloni, 2002)¹² (Qamhieh and Lobaskin 2003)¹³, (Qamhieh and Linse 2005)¹⁴ and theoretically predicted in the limit of strong electrostatic coupling (Naji and Netz 2004)¹⁵. Many theoretical and simulation results are summarized in reviews. (Vlachy 1999)¹⁶, (Bhuiyan et.al. 2002)¹⁷, (Belloni 2000)¹⁸, (Hansen and Lawen 2000)¹⁹.

Monte Carlo simulations within the framework of the primitive model where both colloidal particles and small ions are represented by charged hard spheres and the solvent is treated as a dielectric continuum has been used to investigate intercolloidal structure of colloidal solutions. (Ravindran 2005)⁷, (Qamhieh and Lobaskin 2003)¹³, (Qamhieh and Linse 2005)¹⁴, (A. Naji and Netz 2004)¹⁵, (Messina et.al. 2002)²⁰, (Messina et.al.(july)-2001)²¹. The effect of discrete nature of the macroion charge distribution has been considered in many reviews^{14,20,21}.

Because the Stability of asymmetric electrolytes depends on the balance of attractive van der Waals forces and repulsive interactions which is the interaction between similar charged electric double layers (electrostatic forces). So the distribution of ions in electrical double layer surrounding the charged surface in the solution plays an important part in colloid science and biophysics. Its thickness is a very important parameter, which determines the range of the double layer repulsion.

The characteristics of macroion electric double layer (EDL) have been studied by molecular dynamic methods (Semashko et.al. 2005)²² (Semashko and Brodskaya 2006)²³. A study of a planar EDL in the presence of mixtures of electrolyte is presented via theory and simulation (Molina et.al. 2006)²⁴, (Madurga et.al.2007)²⁵.

In this work Monte Carlo simulations are applied to the investigation of the effect of the surface charge discretization and the counterion size on the EDL in various electrolyte solutions.

The goal of this thesis is to understand the effects of surface charge discretization (mobile charge) on electric double layers, which in turn will affect some properties of solutions containing macroions and their counterions by Monte Carlo simulation using model of uniform and discrete charge distributions. The examination of the distribution of small ions near charged colloids as well as the intercolloidal structure of colloidal solutions is based on the primitive model of electrolytes. In this model, the charged colloids (referred to as macroions) and the small ions are both represented as hard spheres, whereas the solvent is treated as a dielectric medium.

1.1 Colloids

Colloids are defined as very small, finely divided solids (particles that do not dissolve) that remain dispersed in a liquid for a long time due to their small size and electrical charge. The behavior of large objects is governed by gravity while the behavior of very small objects is governed by thermal motion. Colloidal objects will diffuse randomly in response to thermal energy (Brownian motion, bombardment of the particles of the dispersion medium is responsible for this motion) but may also settle out slowly. Milk, wine, clay, dyes, inks, paper and pharmaceuticals are good examples of useful colloidal systems (Roij, 2009)¹, (Shaw, 1992)².

Because of wide range of application of colloidal substances in our life so it is important to study its stability. It was found that bare Coulomb force between the macroions is repulsive, but the presence of microscopic counterions screen the direct Coulomb repulsions (referred to as Coulomb screening). The particles interact via screened coulombic interaction with the range depending on ionic purity. It has been shown that the repulsion between similarly charged particles may be considerably reduced due to correlations among the counterions. There is an attractive force (van der Waals) that molecules exert towards each other.

1.2 Charge inversion (phenomena of over charging)

Charge inversion (counter intuitive phenomenon) occurs when the number of counterions in the vicinity of the macroion surface is so high that the macroparticle bare charge is overcompensated. This gives rise to a strong short range attraction between like-sign charged colloids (Qamhieh and Lobaskin 2003)¹³, (Qamhieh and Linse 2005)¹⁴, (Messina et.al.(july)-2001)²¹, (Molina et.al. 2006)²⁴, (Messina et.al. (March)-2001)²⁶, (Besteman et.al. 2008)²⁷. It is driven by the counterion correlations (that are ignored in mean-field theories), the existence of correlation-induced attraction between charged surfaces of equal sign has important consequences on colloid stability and to provide an explanation for the precipitation occurred after the addition of multivalent ions to solutions or suspensions of macroions. This phenomenon cannot be explained by Mean-field theories (like Poisson–Boltzmann model).

Charge inversion is possible for a variety of systems, ranging from solid surface of mica or lipid membranes to DNA (Sennato et.al 2009.)²⁸. It is of special interest for delivery of genes to living cells for the purpose of gene therapy. The problem is that both bare DNA and a cell surface are negatively charged and repel each other. The goal is to screen DNA in such a way that the resulting complex is positive.

Qamhieh et.al made a computer simulation study of charge inversion in an asymmetric electrolyte treated by multivalent salt. They found that addition of multivalent salt caused macroion aggregation but when the inverted macroion charge becomes large enough the aggregation is redissolved, and enlarging the counterion valence increasing the effect of these phenomena(Qamhieh and Lobaskin 2003)¹³.

Holm et.al. indicated that the charge inversion of EDLs with electrolyte mixtures can be described fairly well by using Integral Equations theories and MC simulations ,they proved that the charge inversion depends on the ionic size chosen in the calculations(Holm et.al. (March)-2001)²⁶.

The theoretical proposal that spatial correlations between ions are the driving mechanism behind charge inversion was supported by experimental result (Besteman et.al. 2008)²⁷. Reversal of the polarity of charged surfaces in water upon the addition of tri- and quadrivalent ions was proved by using atomic force microscopy (Besteman et.al. 2008)²⁷. They found that bulk concentration of multivalent ion salt which charge inversion reversibly occurs depends only very weakly on the chemical composition, surface structure, size and lipophilicity of the ions, but is dominated by their valence.

1.3 Electric double layers

In asymmetric electrolyte solutions there will be accumulation of counterions in the vicinity of macroions because of the strong attractive interaction between a macroion and oppositely charged ions . The small ions that have a charge of the same sign (co-ions) are pushed out of this region. This unequal distribution gives rise to a potential across the interface (Holmberg 2002)²⁹ .

The firmly attached layer of counterions around the surface of the macroion is known as the Stern layer. Additional positive ions are still attracted by the negative macroion, but now they are repelled by the Stern layer as well as by other positive ions that are also trying to approach the macroion. This dynamic equilibrium results in the formation of a diffuse layer of counterions .The point where the Stern layer and the diffuse layer meet is defined as Slip plane (Shear plane). The counterion concentration is high near the surface and gradually decreases with distance, until it reaches equilibrium with the concentration in the solution. But For co-ions they are repelled by the negative macroion because they have the same charge as the macroion. So their concentration will gradually increase with distance, as the repulsive forces of the macroion are screened out by the positive ions, until equilibrium is again reached.

The double layer is formed in order to neutralize the charged colloid and, in turn, causes surface potential (an electrokinetic potential between the surface of the colloid and any point in the mass of the suspending liquid) .It shrinks as the salt concentration increased so ions get close. In practice, this is used to "screen" or reduce the electrostatic interaction. The thickness of the electrical double-layer is a very important parameter, which determines the range of the double layer repulsion.

Zeta Potential refers to the electrostatic potential generated by the accumulation of ions at the surface of the colloidal particle. It is the potential of the surface at the plane of shear between the particle and the surrounding medium as the particle and medium move with respect to each other. Particle charge can be controlled by modifying the suspending liquid. Modifications include changing the liquid's pH or changing the ionic species in solution. It is the potential difference between the ions in the tightly bound layer and the electroneutral region. The pH at which the calculated zeta potential value is zero is called Isoelectric Point (IEP)

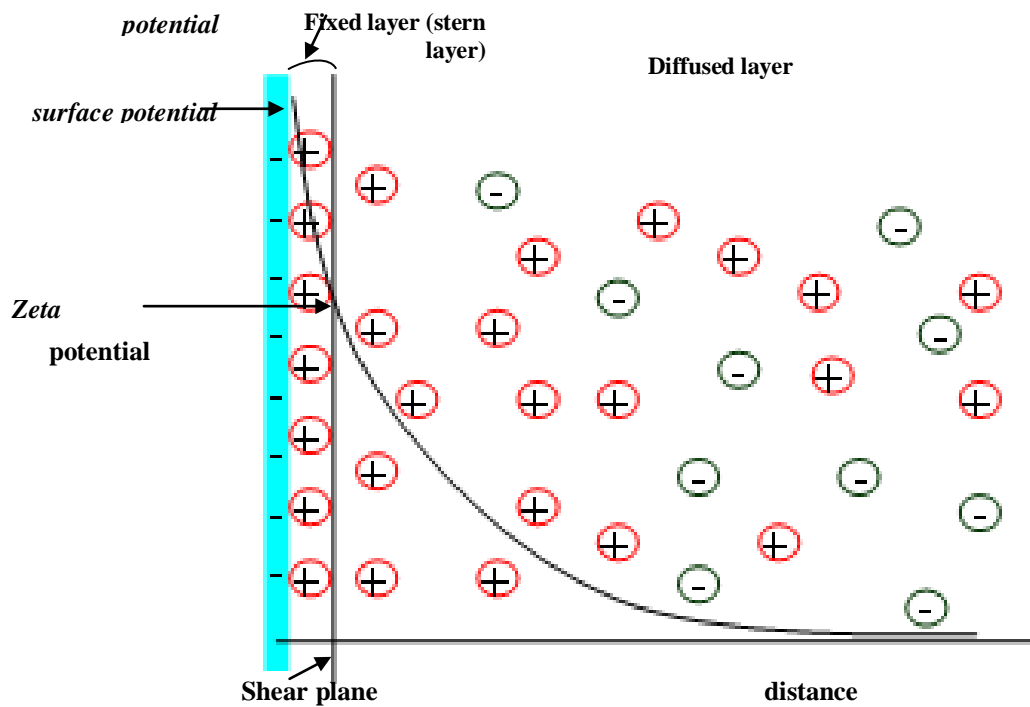


Figure 1.1: Schematic representation of the positions of the Stern plane and the Zeta potential in the electric double layer.

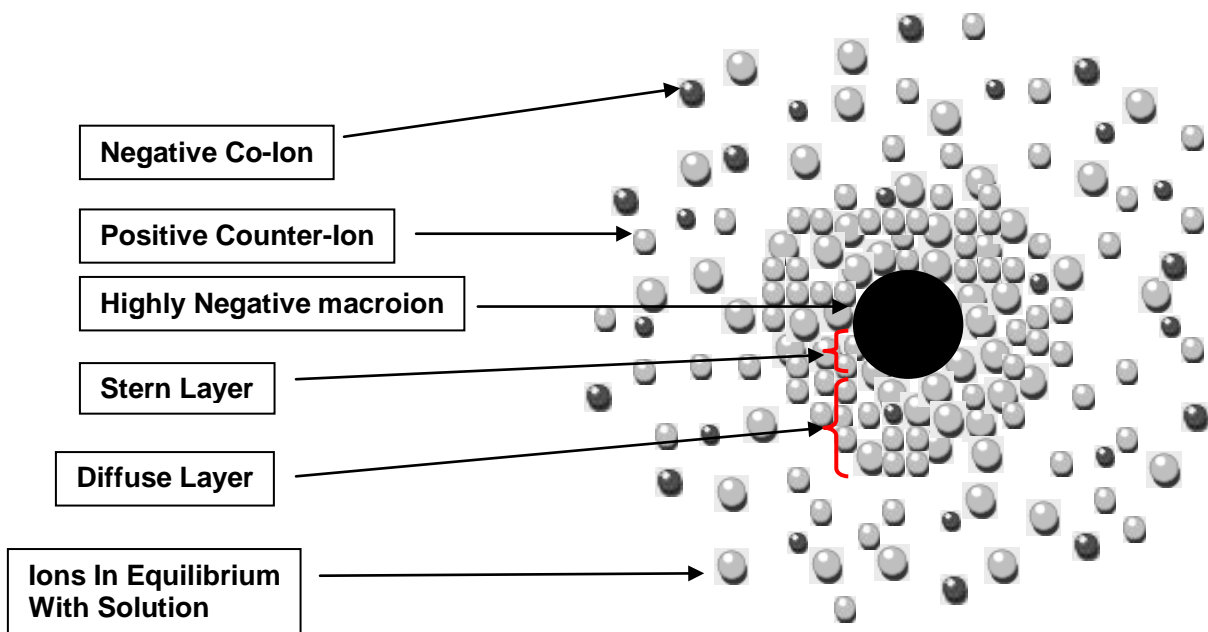


Figure 1.2: The distribution of positive and negative ions around the charged macroion.

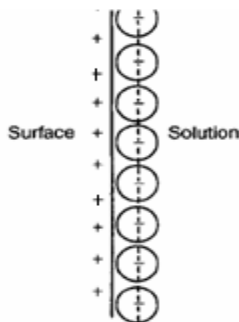
1.4 Models of the electrical double-layer:

Several models have been proposed for the distribution of counterions in the vicinity of the macroion surfaces. (Holmberg 2002)²⁹.

1.4.1 Helmholtz model:

Introduced by von Helmholtz, in which all of the counterions are lined up parallel to the charged surface at a distance of about one molecular diameter. In this model the electrical potential decreases rapidly to zero within a very short distance from the charged surface. Helmholtz model, did not take in consideration the diffusion of the ions in the vicinity of the surface.

a



b

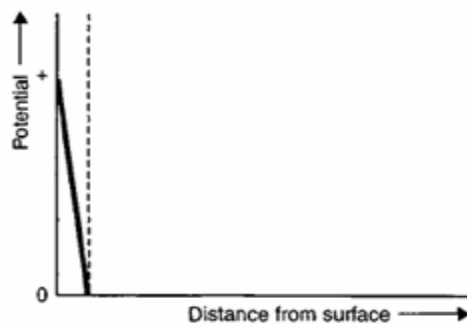


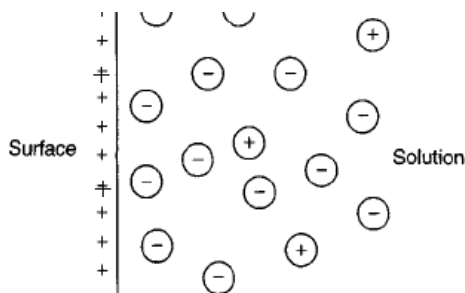
Figure 1.3: Schematic representation of the Helmholtz model of the electrical double-layer: (a) distribution of counterions in the vicinity of the charged surface; (b) variation of electrical potential with distance from the surface. (Holmberg 2002)²⁹

1.4.2 Gouy- Chapman model:

This model was proposed by Gouy and Chapman (Holmberg 2002)²⁹ . It consists of a diffuse distribution of the counterions, with the concentration of such ions falling off rapidly with distance near to the surface because of the screening effect, and then falling off gradually.

Since it treats the ions as point charges and neglects their ionic diameters, it is accurate for planar charged surfaces with low surface charge densities, and distances far away from the surface, but is inaccurate for surfaces with high surface charge densities, especially at small distances from the charged surfaces.

a



b

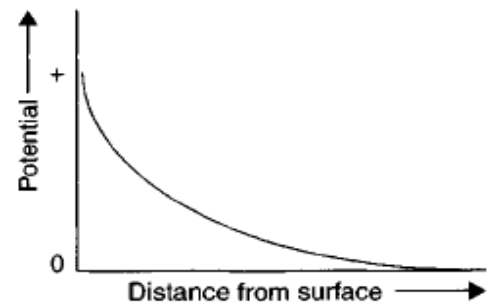


Figure 1.4: Schematic representation of the Gouy-Chapman model of the electrical double-layer: (a) distribution of counterions in the vicinity of the charged surface; (b) variation of electrical potential with distance from the surface. (Holmberg 2002)²⁹.

1.4.3 Stern-Graham model

Stern-Graham model (Holmberg 2002)²⁹, divides the double layer into two parts:

- (i) A fixed layer of strongly adsorbed counterions, adsorbed at specific sites on the surface. This is known as the Stern layer and the potential decays rapidly and linearly in this layer.
- (ii) A diffuse layer of ions similar to that of the Gouy-Chapman model. The potential decay is much more gradual in the diffuse layer. In the case of specifically adsorbing ions (multivalent ions, surfactants) the sign of the Stern potential may be reversed.

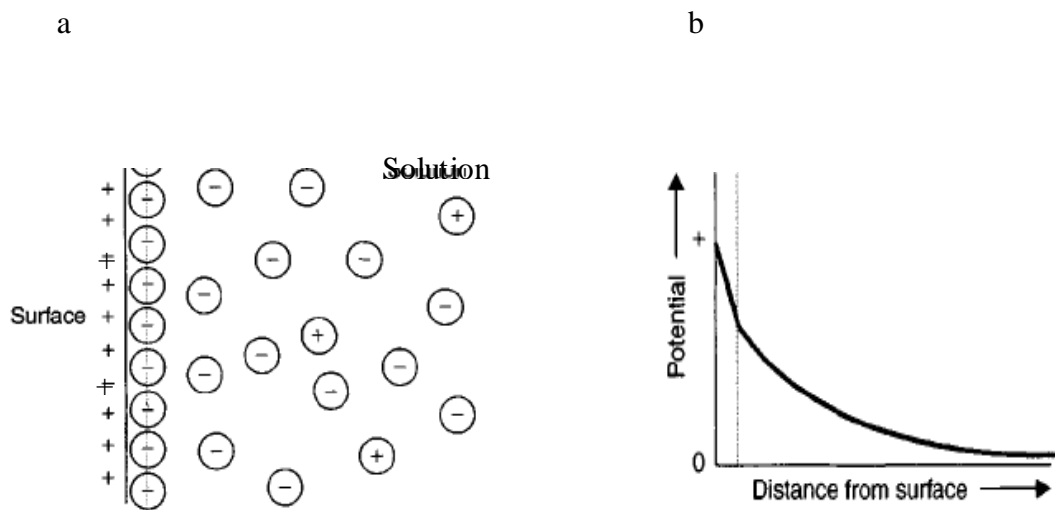


Figure 1.5: Schematic representation of the Stern-Graham model of the electrical double-layer: (a) distribution of counterions in the vicinity of the charged surface; (b) variation of electrical potential with distance from the surface. (Holmberg 2002)²⁹.

1.5 DLVO theory

Encounters between particles occur as a result of Brownian motion and stability of a suspension is determined by the interaction between particles during these encounters. This stability depends on the balance of attractive van der Waals forces and repulsive interactions which is the interaction between similar charged electric double layers (electrostatic forces). In small distance van der Waals forces between particles is more powerful than electrostatic coulomb repulsion forces.

Derjaguin and Landau, and Verwey and Overbeek developed a quantitative theory for the stability of lyophobic colloids, known as DLVO theory (Bjerrum, et.al. 1926)⁴, (Deryaguin et.al. 1941)⁵. In this theory, the van der Waals attraction (short range attractions) is combined with the double-layer repulsion (electrostatic repulsion) and an energy–distance curve can be established to describe the conditions of stability/instability.

An essential ingredient of the DLVO theory is BP a mean-field approximation that neglects counterion-counterion correlations, and treats the free ions (counterions and added salt) as point-charge. It is accurate, for monovalent ions. However, for multivalent ions the BP equation becomes less accurate

Based on a Debye–Hückel analysis, the ‘DLVO’ state that the role of the ions is to form a double layer around each colloid and to screen the repulsive interaction between polyions at large separation.

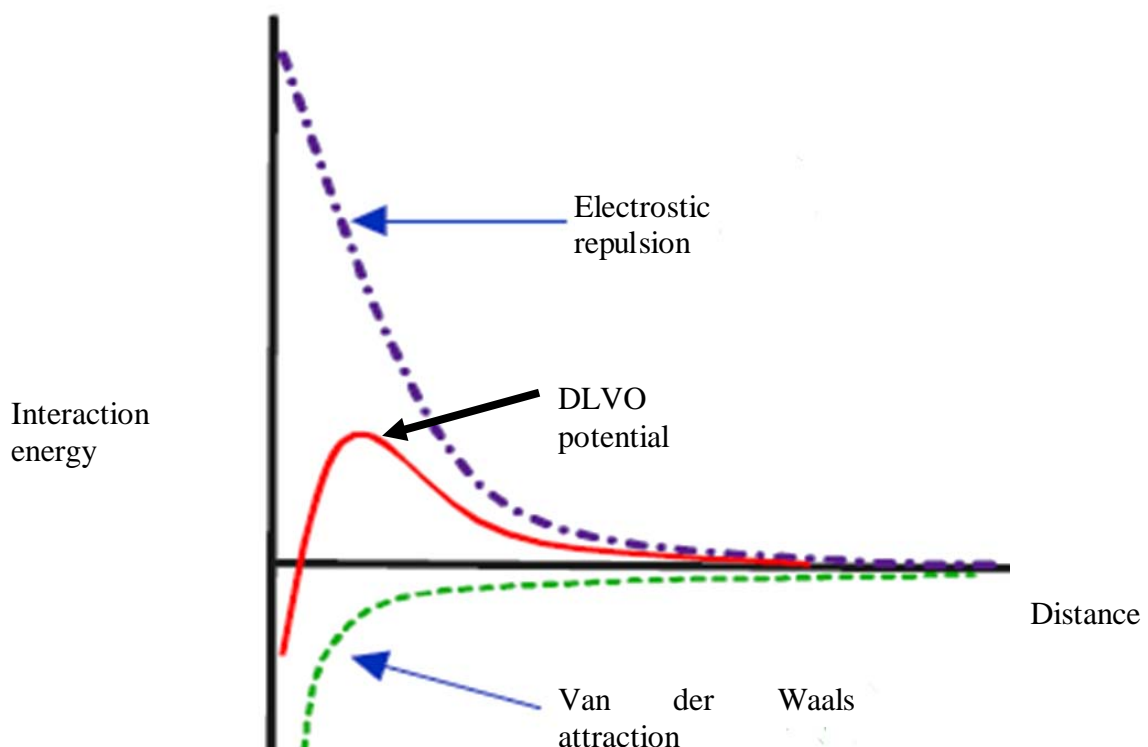


Figure 1.6: DLVO-type interaction (continuous line) obtained as the sum of the electrostatic repulsion and van der Waals attraction.

1.6 Computer simulations:

A computer simulation (or "sim") is an attempt to model a real-life or hypothetical situation on a computer so that it can be studied to see how the system works. By changing variables, predictions may be made about the behavior of the system. Computer simulation has become a useful part of modeling many natural systems in physics, chemistry and biology, and human systems in economics and social science (the computational sociology) as well as in engineering to gain insight into the operation of those systems (Allen and Tildesley 2001)³⁰.

A good example of the usefulness of using computers to simulate can be found in the field of network traffic simulation. In such simulations, the model behavior will change each simulation according to the set of initial parameters assumed for the environment. Traditionally, the formal modeling of systems has been via a mathematical model, which attempts to find analytical solutions enabling the prediction of the behavior of the system from a set of parameters and initial conditions.

Computer simulation is often used as an adjunct to, or substitution for, modeling systems for which simple closed form analytic solutions are not possible. There are many different types of computer simulation, the common feature they all share is the attempt to generate a sample of representative scenarios for a mode in which a complete enumeration of all possible states would be prohibitive or impossible.

Computer simulations have a valuable role to play in providing essentially exact results for problems in statistical mechanics which would otherwise only be soluble by approximate methods or might be quite intractable. Statistical thermodynamics links the interactions on the molecular level to the macroscopic properties of the system. The basic concept of Statistical thermodynamics is the ensemble. Members of ensemble have some constraints which are specific for that ensemble. These constraints thermodynamically describe the system completely. Several software packages exist for running computer-based simulation modeling (e.g. Monte Carlo simulation) that makes the modeling almost effortless.

It is a technique which has been used to improve our understanding of phase transition and behaviors at interfaces. The results of computer simulation may also be compared with those of real experiments. Experiments deal with real systems, which might be more or less complicated, while theories involve approximate solutions of models. computer simulations are, thus, a useful tool for bridging the gap between the two (Allen and Tildesley 2001)³⁰.

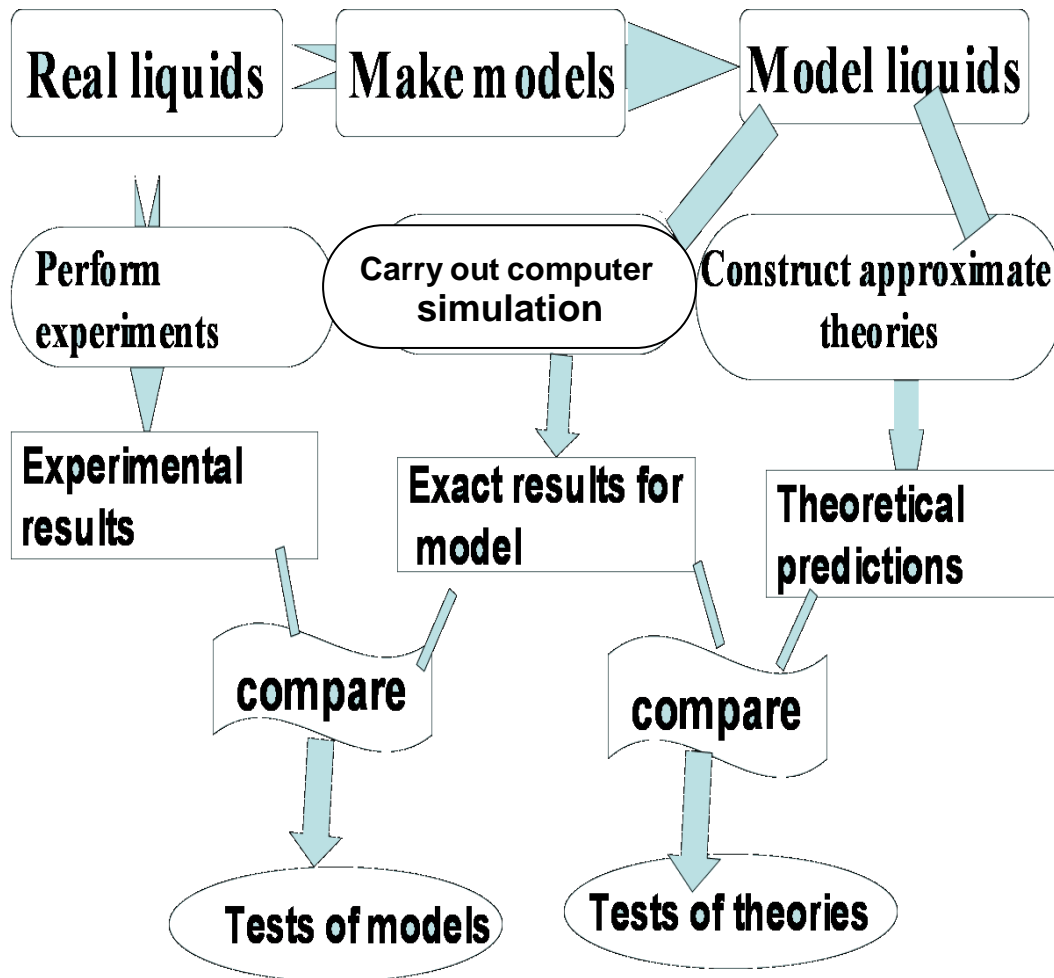


Figure 1.7: The connection between experiment ,theory ,and computer simulation (Allen and Tildesley 2001)³⁰

1.7 Statement of the problem

The goal of the thesis is to understand the effects of surface charge discretization (mobile charge) on electric double layers, which in turn will have an effect on some properties of solutions containing macroions and their counterions.

The thesis is organized as follows: Chapter one contain the introduction. Chapter two describes the method and model settings for the simulations. Chapter three gives a detailed account of the results and discussion. And the conclusions are given in the final chapter.

Chapter Two

Model and Method

2. MODEL AND METHOD

2.1 Method

The method which has been used to study the effect of the charge distribution and counterions size on the properties of electric double layer is Monte Carlo (MC) simulation, in the canonical ensemble, at constant number of particles, volume, and temperature according to the standard Metropolis algorithm. The configurations were generated by first placing the macroion in the center of the spherical cell. The macroion charges were positioned according to the different charge distributions. Finally, the counterions were positioned randomly. 2×10^6 attempted MC moves per particles were made in the production runs. All the simulations were performed using the integrated Monte Carlo/molecular dynamics/ Brownian dynamics simulation package MOLSIM. (Linse 2004)³¹

2.2 Monte Carlo Simulation

Monte Carlo simulation is a technique which has had a great impact in many different fields of computational science. This technique derives its name from the casinos in Monaco city (famous for its casino) where games of chance involve repetitive events with known probabilities. A random numbers used to model some sort of a process. This technique works particularly well when the process is one where the underlying probabilities are known but the results are more difficult to determine.

It is a stochastic technique (meaning it is based on the use of random numbers and probability statistics to investigate problems). You can find MC methods used in everything from economics to nuclear physics to regulating the flow of traffic. Of course the way they are applied varies widely from field to field, and there are dozens of subsets of MC even within chemistry. But, strictly speaking, to call something a "Monte Carlo" experiment, all you need to do is use random numbers to examine some problem. Monte Carlo simulation was invented by scientists working on atomic bomb in the 1940s, who named it for the city in Monaco famed for its casinos and games of chance. Its core idea is to use random samples of parameters or inputs to explore the behavior of complex system or process. The scientists faced physics problems such as models of neutron diffusion, which were too complex for an analytical solution, so they had to be evaluated numerically, by using MC Simulation. To get more accurate approximations you should perform more simulations, this is can happen because computers are now able to perform millions of simulations much more efficiently and quickly than before.

Table 2.1: Name of the ensemble used in simulation.

constraint	Name of the ensemble	states
NVE	Micro-canonical	Constant number of particles ,volume and energy
NVT	Canonical	Constant number of particles ,volume and temperature
NPT	Isothermal-isobaric	Constant number of particles, pressure and temperature

The use of MC methods to model physical problems allows us to examine more complex systems than we otherwise can. Solving equations which describe the interactions between two atoms is fairly simple; solving the same equations for hundreds or thousands of atoms

is impossible. With MC methods, a large system can be sampled in a number of random configurations, and that data can be used to describe the system as a whole.

"Hit and miss" integration is the simplest type of MC method to understand. A MC experiment which calculates the value of pi is based on a "hit and miss" integration. We can estimate(pi) by Hit and miss method as seen in figure 2.1 . Its idea is that we find some region in space of known volume which encloses the volume we want to integrate, then generate random points everywhere in this region ,and count the points which actually do hit the volume we want to handle. . By increasing the number of simulations, we can increase the accuracy and also the time taken to complete the process.

Estimation of (pi)

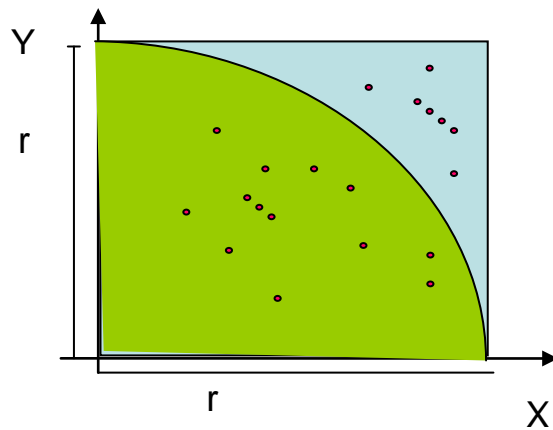


Figure 2.1: Estimation of π

$$\text{Area of shaded area} = \frac{\pi r^2}{4}$$

$$\text{Area of square} = r^2$$

$$\frac{\text{\# darts hitting shaded area}}{\text{\# darts hitting inside square}} = \frac{\text{Area of shaded area}}{\text{Area of square}}$$

$$\frac{\text{\# darts hitting shaded area}}{\text{\# darts hitting inside square}} = \frac{\frac{\pi r^2}{4}}{r^2} = \frac{\pi}{4}$$

$$\pi = 4 \frac{\text{\# darts hitting shaded area}}{\text{\# darts hitting inside square}}$$

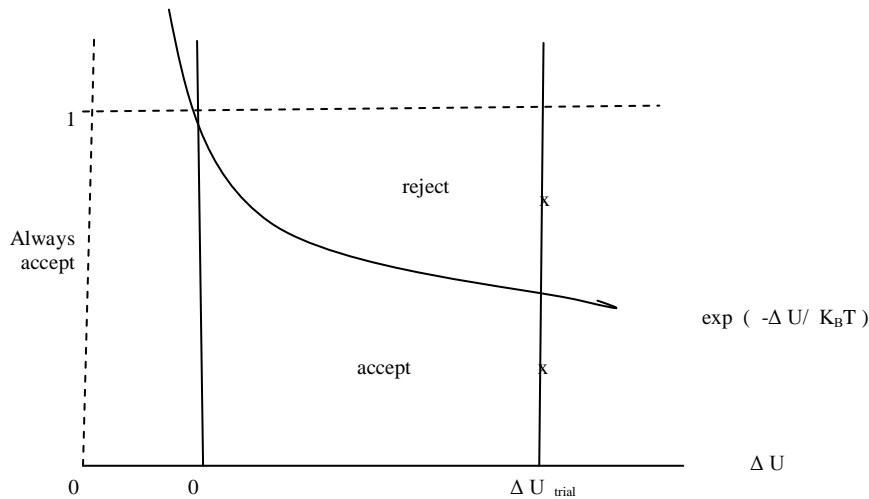
2.2.2 Metropolis algorithm:

In the Metropolis algorithm, the phase is sampled in such a way that configuration contribute significantly to the configurationally integral are visited more frequently than those that only contribute little to it. Acceptance and rejection of MC trial move are chosen

in away that produces a Markov chain. It is implemented using the following algorithm:

- 1- Chose the particles to move at random and move them by a (random) distance.
- 2- Calculate the energy difference $\Delta U_{trial} = U_{new} - U_{old}$ between the old and the new configuration.
- 3- If $\Delta U_{trial} \leq 0$ accept the new configuration, else if random number generating $0 \leq x \leq 1$ is smaller than $\exp(-\Delta U_{trial} / K_B T)$, accept the move, else reject the move and count the old configuration as the new configuration.

After every step , data for the averages is accumulated ,before a new trial move is attempted(go back to point1).The acceptance probability \hat{w} in step 3 can be written as



$$\hat{w}(\mathbf{r}_{i,old} \rightarrow \mathbf{r}_{i,new}) = \min[1, \exp(-\Delta U_{trial} / K_B T)]$$

Figure 2.2: Metropolis algorithm is used to reject or accept a move.

A Markov chain is a sequence of trials, which satisfies two conditions (1) the outcome of each trial belongs to a finite set of outcomes (2) the outcome of a trial just depends on trial that immediately precedes it .

2.3 Model

Monte Carlo simulation performed was based on a primitive model of electrolyte solutions used in the framework of Mc-Millan–Mayer theory. The solvent is treated as a dielectric medium solely characterized by its relative permittivity ϵ_r equal to that of bulk water at T 298K. Whereas the colloids (later referred to as macroions), the counterions, cations and anions are represented by charged hard spheres.

The system under consideration is an asymmetrical electrolyte solution made up of highly charged macroion and small ions. Throughout, macroion are represented as hard sphere with radius $R_M = 20 \text{ \AA}$ and a total charge $Z_M = -60$, originating from $N_S = 60$ charged sites with radius R_S and charge $Z_S = -1$.

The counterions are represented by charged hard spheres with radius $R_i=1 \text{ \AA}$, 2 \AA , 3 \AA and charge $Z_i= +1$, $+2$, or $+3$. The salt represented by hard spheres with radius $R_{ca}=2 \text{ \AA}$ and charge $Z_{ca}= +3$ for cations, and $R_a=2 \text{ \AA}$ and charge $Z_a= -1$ for anions.

Three different types of macroion charge distributions have been considered:

1- Continuous surface charge distribution (the uniform macroion charge distribution) called central (c) charge distribution; all N_S charges are localized at the center of the macroion. As to the electrostatic field at $r>R_M$, by Gauss theorem this charge distribution is equivalent to a homogeneous surface charge density $\sigma_M=eZ_M/4\pi R_M^2$ at $r=R_M$ see figure 2.3. a.

2- Mobile surface (ms) charge distribution, the N_S charges are positioned at the distance $r_S=R_M$ from the center of the macroion, hence the macroion charges are exactly localized (have no extension, i.e., $R_S=0$) on the hard-sphere surface of the macroion, and thus the macroion surface is smooth see figure 2.3. b.

3- Mobile protruding (mp) charge distribution, the N_S charges are positioned at the distance $r_S=R_M+R_S$ from the center of the macroion with $R_S=2 \text{ \AA}$, where R_S is also the hard-sphere radius of the macroion charges.

Hence, the macroion charges are positioned 2 \AA outside the hard-sphere surface and are protruding 4 \AA into the solution see figure 2.3. c.

In the mobile (m) arrangement, the charges are laterally mobile at the distance r_S . The characteristic separation between two neighboring macroion charges becomes $\approx 8 \text{ \AA}$.

A spherical cell boundary condition has been used with radius $R_{sph}=100 \text{ \AA}$ ($5R_M$) containing one macroion ($N_M=1$) at the center of the cell. The macroion is held fixed and is located at the center of the cell. To avoid image charge complications, the permittivity ϵ_r is supposed to be identical within the whole cell.

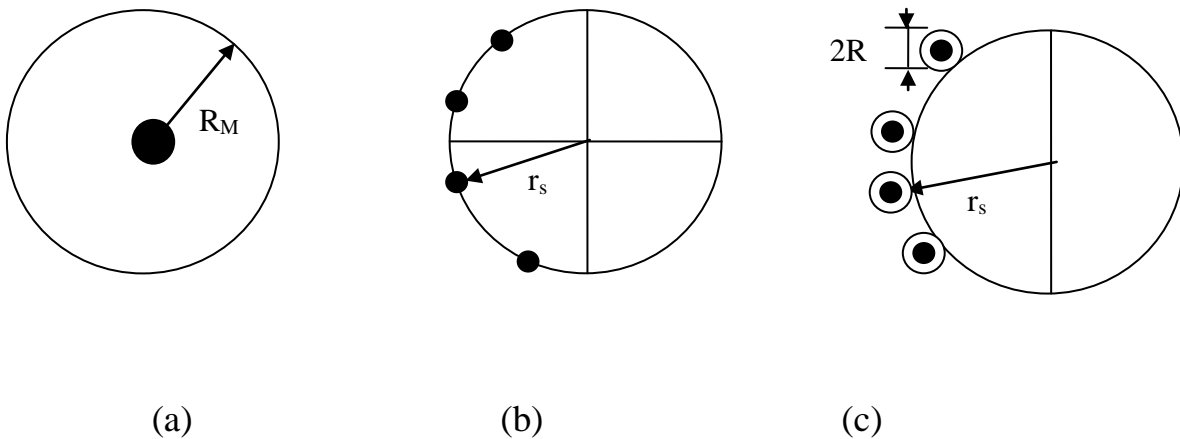


Figure 2.3: Schematic illustration of the macroion charge distributions: (a) a central charge with R_M denoting the macroion radius, (b) point charges on the macroion surface, and (c) protruding charges with hard-sphere radius R_S . The r_S denotes the radial location of the macroion charge.

The total potential energy of the system U is:

$$U = U_{\text{hs}} + U_{\text{elec}} + U_{\text{ext}} \quad (1)$$

Hard-sphere repulsion U_{hs} is given by:

$$U_{\text{hs}} = \sum_{I < j} u_{Ij}^{\text{hs}}(r_{Ij}) \quad (2)$$

With

$$u_{Ij}^{\text{hs}}(r_{Ij}) = \begin{cases} \infty, & r_{Ij} < R_I + R_j \\ 0, & r_{Ij} \geq R_I + R_j \end{cases} \quad (3)$$

With R_I denoting the radius of particle I (a macroion, a macroion site, or a counterion, coion and anion) and r_{Ij} the distance between the centers of particles I and j.

The Coulomb interaction U_{elec} is

$$U_{\text{elec}} = \sum_{I < j} u_{Ij}^{\text{elec}}(r_{Ij}) \quad (4)$$

With

$$u_{Ij}^{\text{elec}}(r_{Ij}) = \frac{Z_i Z_j e^2}{4\pi\epsilon_0\epsilon_r r_{Ij}} \quad (5)$$

Where Z_I is the charge of particle I (a macroion site or a counterion, coion and anion), e the elementary charge, ϵ_0 the permittivity of vacuum, and ϵ_r the relative permittivity of water.

Confinement potential energy U_{ext} is equal to

$$U_{\text{ext}} = \sum_I u^{\text{ext}}(r_I) \quad (6)$$

with

$$u^{\text{ext}}(r_I) = \begin{cases} 0, & r_I \leq R_{\text{sph}} \\ \infty, & r_I > R_{\text{sph}} \end{cases} \quad (7)$$

Throughout, the system is considered at the macroion number density $M=2.510 \cdot 10^{-7} \text{ \AA}^{-3}$, corresponding to a macroion volume fraction $M=0.0084$. The temperature $T=298 \text{ K}$ and the relative permittivity $=78.5$ were used. At these conditions, the Bjerrum length, denoting the

distance between two unit charges at which the Coulomb interaction is equal to the thermal energy, becomes 7.15 Å.

Chapter Three

Results and

Discussion

3 Results and discussion

3.1 Effect of valence and discretization

Macroion-counterion radial distribution functions (rdfs) for the uniform and discrete charge distributions with different counterion valences are shown in Figure 3.1. Such rdfs obtained from a spherical cell describe the distribution of counterions near a single macroion ($g_{mi}(r)$) that is well separated from other macroions. They provide the relative density of small ions at distance r from the macroion, its value being unity in the absence of any spatial correlations. Independent of the counterion valence, there is strong accumulation of the counterions near the macroion surface.

The equilibrium counterion distribution is a compromise between:

- (i) The macroion-counterion electrostatic attraction striving to a complete adsorption of the counterions on the macroion surface.
- (ii) The counterion entropy promoting a homogeneous counterion density.

The counterion valence increases When the macroion-counterion electrostatic increases in magnitude leading to a more uneven counterion distribution. As shown in figure 3.1 the correlation between trivalent ions and macroion is much stronger than the correlation in case of divalent counterions which is stronger than correlation between monovalent ions and macroion. The effect of changing the surface charge distribution from the central to mobile distribution becomes more pronounced as the counterion valence is increased.

In figure 3.2 the counterions approach the surface more closely in case of mobile surface compared to the continues charge distribution. This is related with their stronger electrostatic interaction with the macroion. While in case of mobile protruding the excluded volume effect gave rise to a reduced accumulation of counterions near the macroion.

Figure 3.3 demonstrates the counterions around the macroion and how this accumulation increases by increasing the valence of counterions and as a result the thickness of electric double layer decreases.

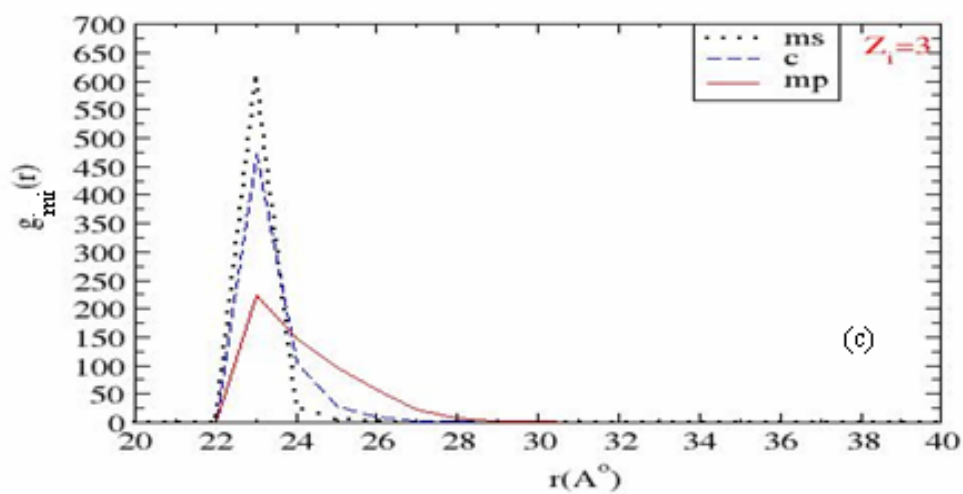
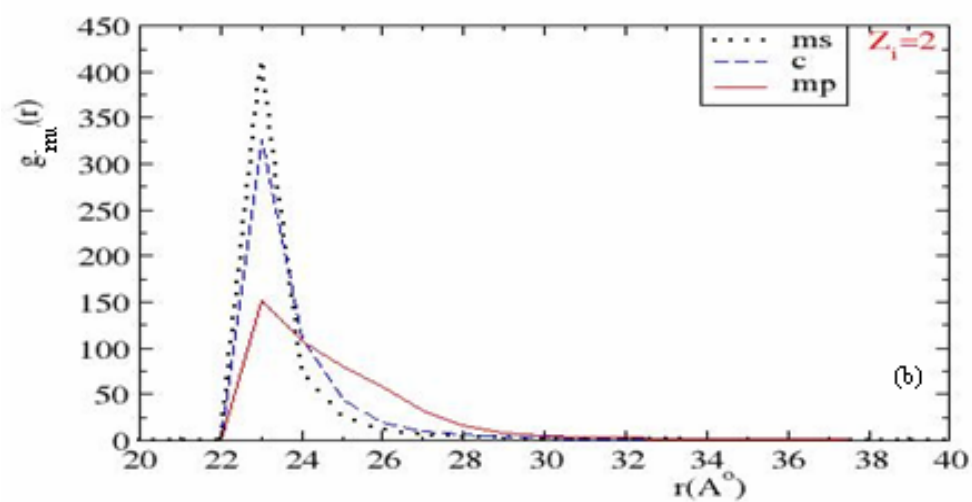
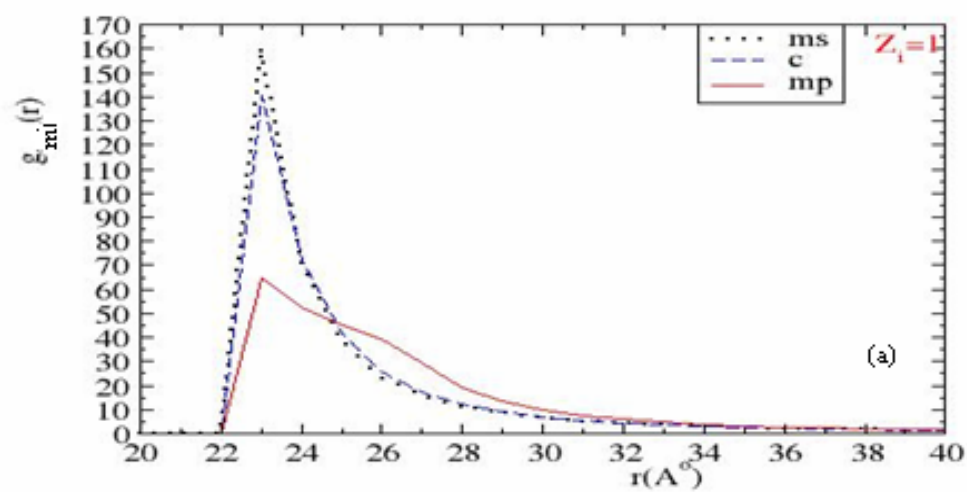


Figure 3.1: Macroion-counterion radial distribution functions at counterion valences (a) $Z_i = 1$, (b) $Z_i = 2$, (c) $Z_i = 3$ for central charge (c) distribution ----- (dashed curve), mobile point (ms)..... (dot curve) and mobile protruding (mp) Charge distribution_____.

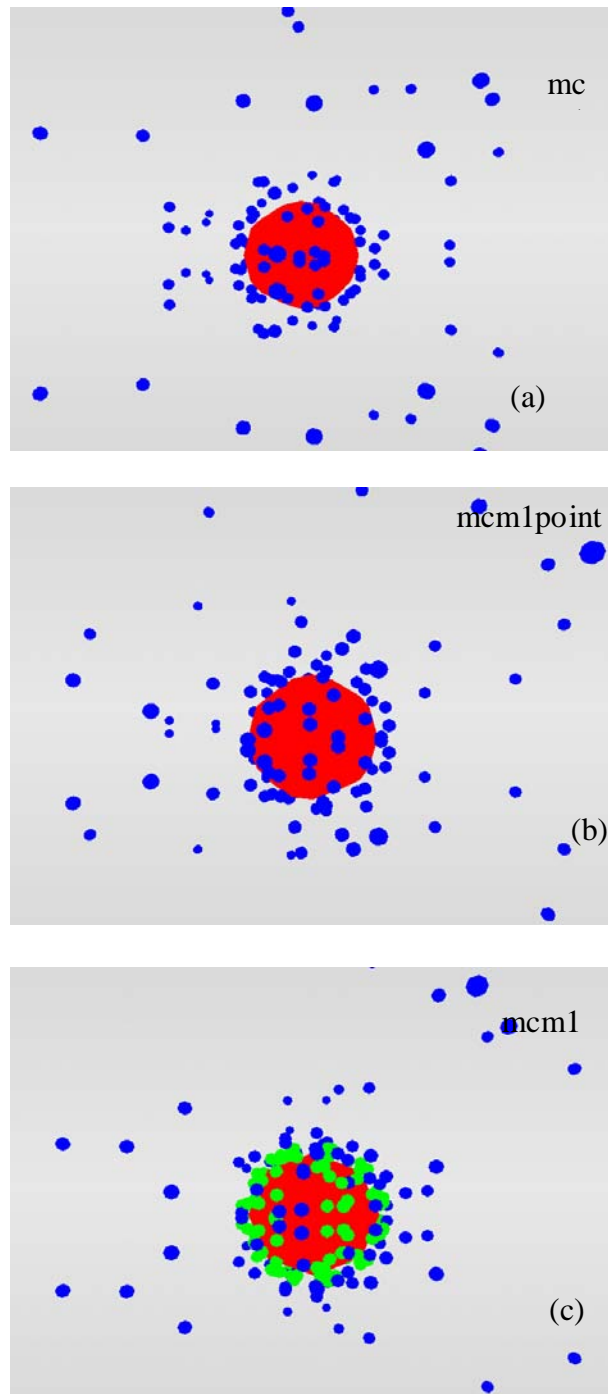


Figure 3.2: Snapshots of systems containing one macroion (red sphere), monovalent counterions (blue sphere), protruding charges (Green sphere) at $Z_i = 1$ in case of (a) central charge distributions, (b) mobile point charge distributions and (c) mobile protruding charge distributions, all particles are enclosed in spherical cell.

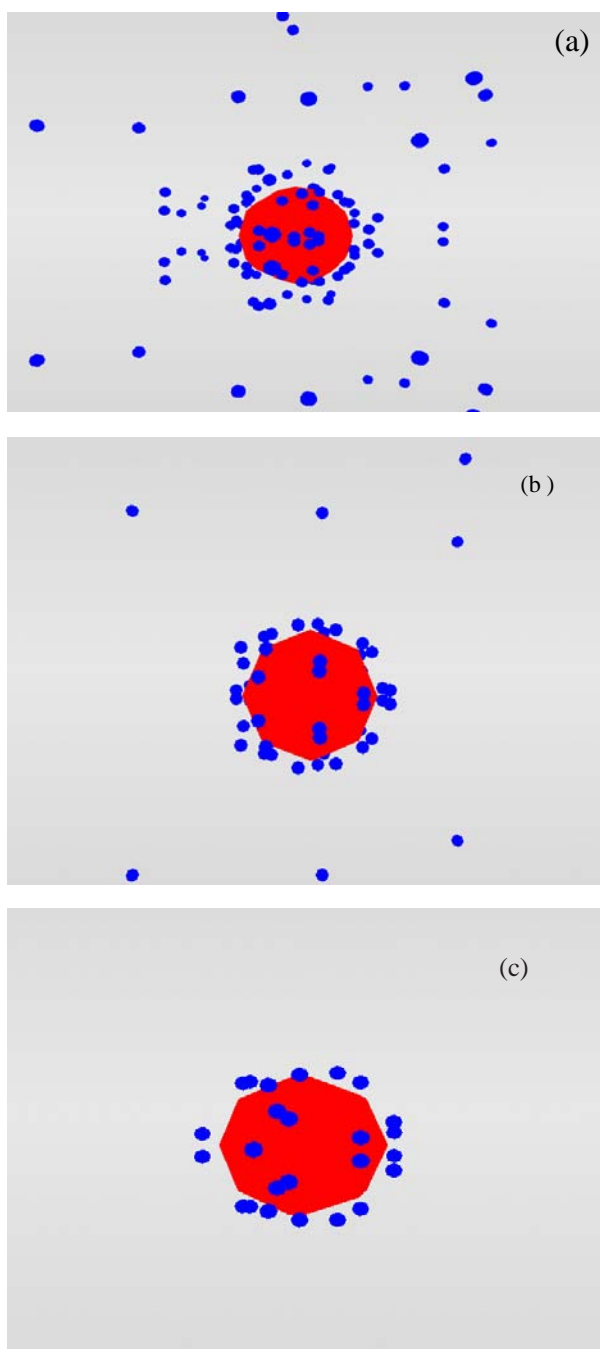


Figure 3.3: Snapshots of systems containing one macroion (red sphere) ,monovalent counterions (blue spheres) at different valences of counterions (a) $Z_i = 1$ (b) $Z_i = 2$ (c) $Z_i = 3$ from central charge distributions.

The maximum accumulation g_{mi} are given in table 3.1, with protruding charges the maximum value is less than the continuous, because of the excluded volume effect dominates over the increased correlation ability. But with point charges distribution, counterions become stronger accumulated to the macroion and the effect increases with counterion valence. For all counterion valences the g_{mi} in mobile surface charge distribution system are larger than in central one which are more than mobile protruding charge distribution . And as increasing the valences the g_{mi} increases for all charge distribution system.

Table 3.1: Values of the maximum accumulation of counterions g_{mi} in the vicinity of macroion for all charges distributions at counterion valence $Z_i = 1, 2$ and 3 .

	central charge distribution	Mobile surface charge distribution	Mobile protruding charge distribution
$Z_i=1$	140	160	64
$Z_i=2$	327	419	150
$Z_i=3$	470	603	220

To describe the fraction of ions appearing within a distance r from the macroion center it is favorable to consider normalized ion running coordination number $P(r)$. It is used to facilitate a comparison among different ions valences,

$$P(r) = \text{rcn}(r) / N_i$$

Eq. 1

And it possesses the limit $\text{rcn}(r) \rightarrow N_i$ as $r \rightarrow R_{\text{sph}}$.

R_{sph} radius of the spherical cell, N_i is number of counterions.

Where rcn is the running coordination number follows directly from the macroion- radial distribution function according to

$$\text{rcn}(r) = \rho_i \int_0^r 4\pi r'^2 g_{\text{mi}}(r') dr'$$

Eq. 2

Where ρ_i is the uniform ion number density, g_{mi} is the macroion- ions radial distribution function.

We calculated $P(r)$ for the counterions by using eq.1; the results are shown in Figure 3.4.

Relative normalized running coordination number for the counterions is shown in figure 3.5. It shows the difference of the fraction of counterions near the surface between the central and discrete charge distribution.

$$\Delta P(r) = P(r) - P_{\text{central charge}}(r).$$

Eq.3

The figure shows the increased accumulation of the counterions for the surface charge distribution and the opposite behavior for the protruding charge distribution. This effect increases with increasing Z_i . The deviations from the central charge distribution are mainly localized to the nearest $\approx 10 \text{ \AA}$ from the macroion surface. But for longer distances the differences in the integrated number of counterions are smaller.

Changing of the conventional central charge distribution with more realistic macroion charge distributions considerably affect the counterion distribution near a macroion. The accumulation of counterions increases in the case of surface charges because of the increased macroion-charge-counterion correlation. But in the case of protruding charges the excluded volume effect dominates over the correlation effect. The described effects become more prominent with increasing counterion valence.

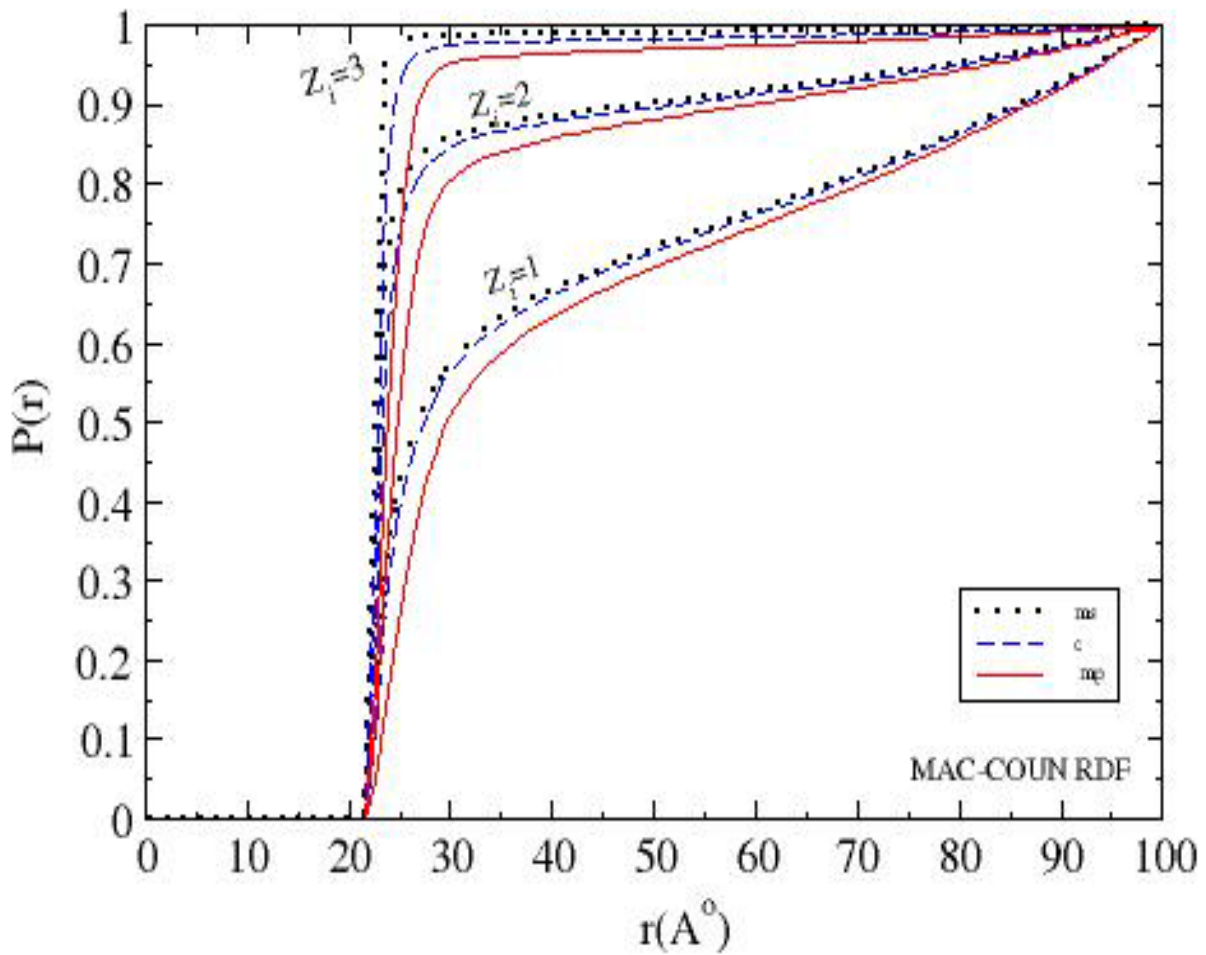


Figure 3.4: Normalized counterion running coordination number $P(r)$ at counterion valences $Z_i= 1, 2, 3$ for central charge distribution (c) ----- (dashed curve), mobile point (ms)..... (dote curve) and mobile protruding (mp) _____ charge distributions.

Using 3 \AA as a distance criterion (Qamhieh and Linse 2005)¹⁴, and from figure 3.4, the values of the counterions at the macroion surface are listed in table 3.2 for different counterion valences and at all charge distribution models. The table demonstrates the strong effect of the counterion valence on the association of the counterions to the macroion. These values mean for example for central they are 40%, 73%, and 93%, with mono-, di-, and trivalent counterions respectively, of the counterions are at the macroion surface.

Table 3.2: Ratio of counterions at $r= 25\text{\AA}$ for all charge distributions model for different counterions valences.

Counterion valences.	central charge distribution	Mobile surface charge distribution	Mobile protruding charge distribution
$Z_i=1$	40%	42%	26%
$Z_i=2$	73%	79%	54%
$Z_i=3$	93%	97%	73%

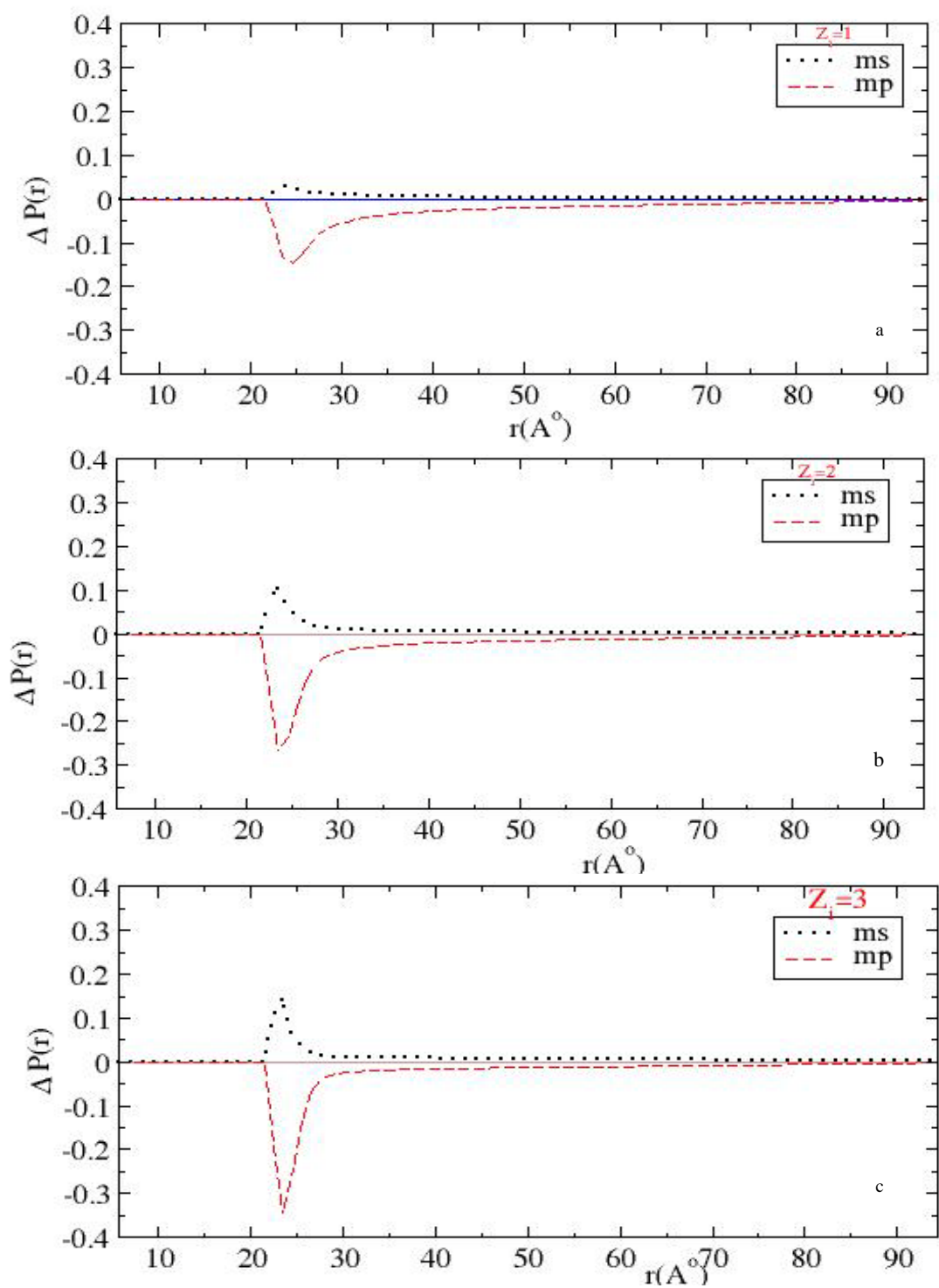


Figure 3.5: Relative normalized running coordination number at counterion valences (a) $Z_i=1$, (b) $Z_i=2$, and (c) $Z_i=3$ for the mobile surface and mobile protruding charge distributions as obtained from the spherical cell. $\Delta P(r) = P(r) - P_{\text{central charge}}(r)$.

Local charge density, of any ion, $\rho(r)$ in Coulomb per centimeter cubic can be calculated from rdfs by using eq. 4 and eq. 5, it means how many charges in the volume at the vicinity of the macroion. Figure 3.6 presents the local charge density of counterions for continuous and discrete models of macroion charges distributions in the absence of background electrolyte at different valences. The values in the table are the maximum value for all charge distributions at 25\AA at counterion radius $=2\text{\AA}$. Demonstrate how the valence and discretization affected the charge density in the EDL. Its value increases and its dispersion decreases by increasing the valence and its value in mobile surface charge distribution is more than in case of central charge distribution.

$$\rho(r) = \rho_i g_{mi} \quad \text{Eq.4}$$

$$\rho_i = N_i Z_i e / (4/3 \pi R_{sph}^3) \quad \text{Eq.5}$$

Where $\rho(r)$ is the local charge density of ion, ρ_i is the uniform counterion number density, g_{mi} is the macroion-ions rdfs, N_i is the number of ions, Z_i is the charge of the ions, and e is the elementary charge.

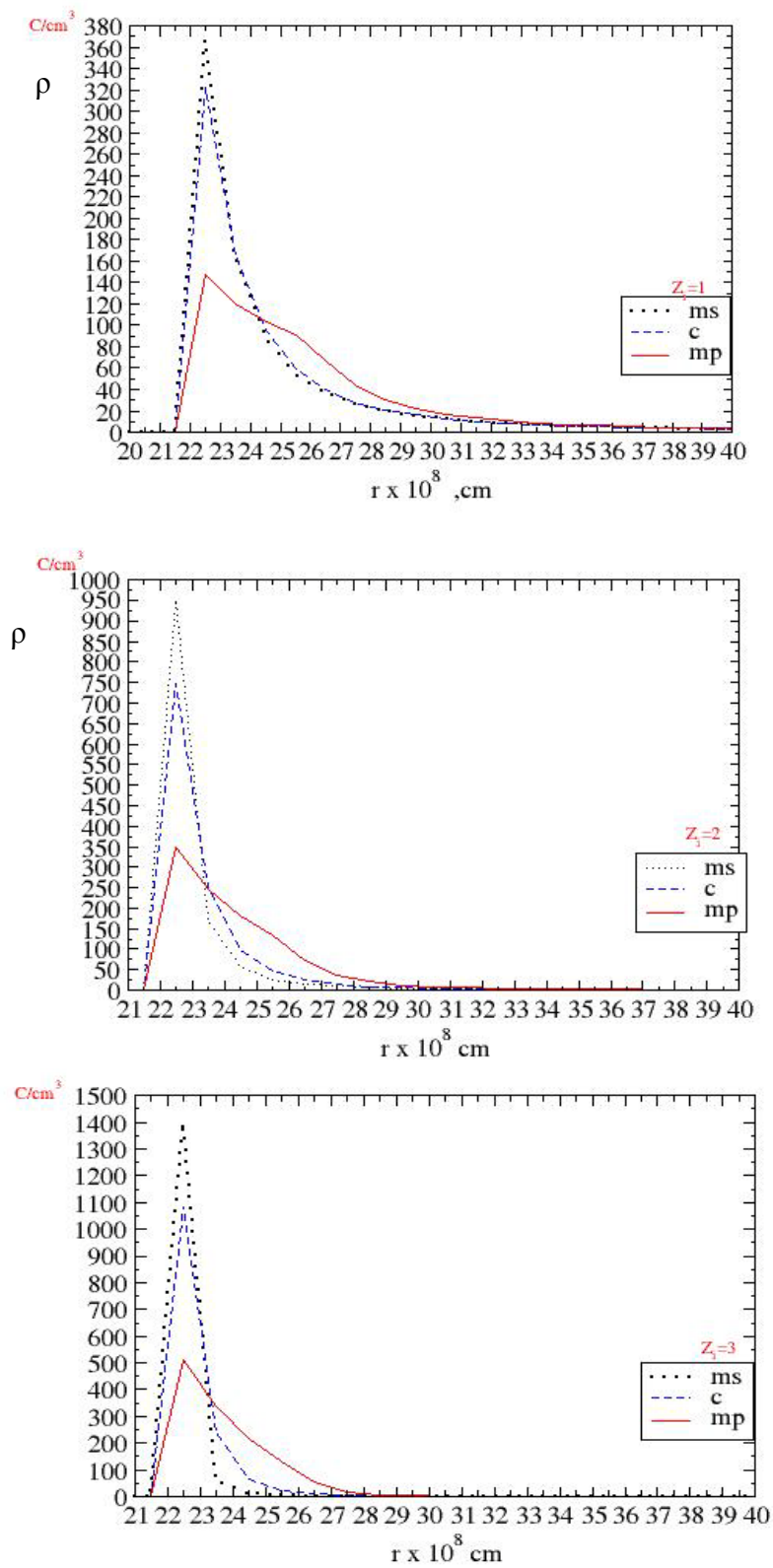


Figure 3.6: local charge density at $Z_i = 1, 2,$ and 3 for the system with discrete and central charge distributions

From figure 3.6 we obtain values of maximum local charge density as seen in table 3.3 demonstrating how the valence and discretization affected the charge density in the EDL. Its value increases by increasing the valence and its value in mobile surface charge distribution is more than in case of central charge distribution.

Table 3.3: Maximum local charge density ($\rho(r)$ in C/cm^3) accumulation of counterions in the vicinity of macroion for all charges distributions at different counterion valence.

Counterion valences	Central charge distribution	Mobile surface charge distribution	Mobile protruding charge distribution
$Z_i=1$	322	366	148
$Z_i=2$	747	942	346
$Z_i=3$	1083	1400	510

The effect of valence and discretization on accumulated charge has been determined as in figures 3.7 and 3.8. Accumulated charge (Z_{acc}) is the net charge of macroion, as well as counterions and coions bound to the macroion

$$Z_{acc} = Z_M + \sum (Z_I q_I)$$

Eq.6

Z_{eff} is Z_{acc} at $r = 25\text{\AA}$

Z_I is the charge of any ion (counterion, coion, or cation) q_I is the charge of any ion. For all counterion valences the effect of discretization is seen in figure 3.7, at the surface of macroion at $r = 25\text{\AA}$ the value in the case of mobile protruding is less than the others, this is because of the volume of the charge. In the case of $Z_i = 1$ the accumulated charge for mobile point = -56, for central = -57 and for mobile protruding = -59. As the counterion valence increases the accumulated charge increases as in figure 3.8.)

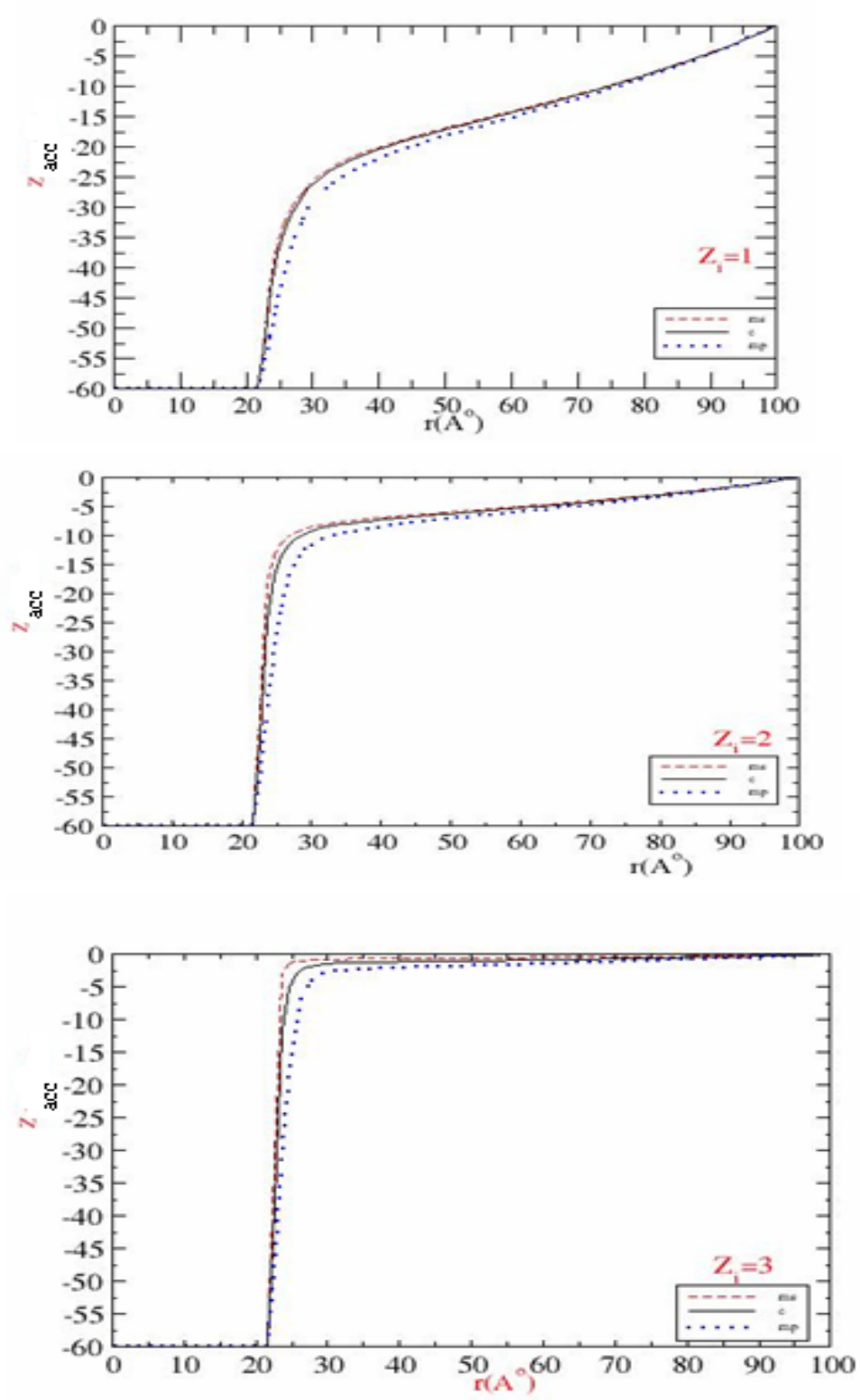


Figure 3.7: Accumulated charge at $Z_i = 1, 2, 3$ for the systems with central and discrete charge distributions.

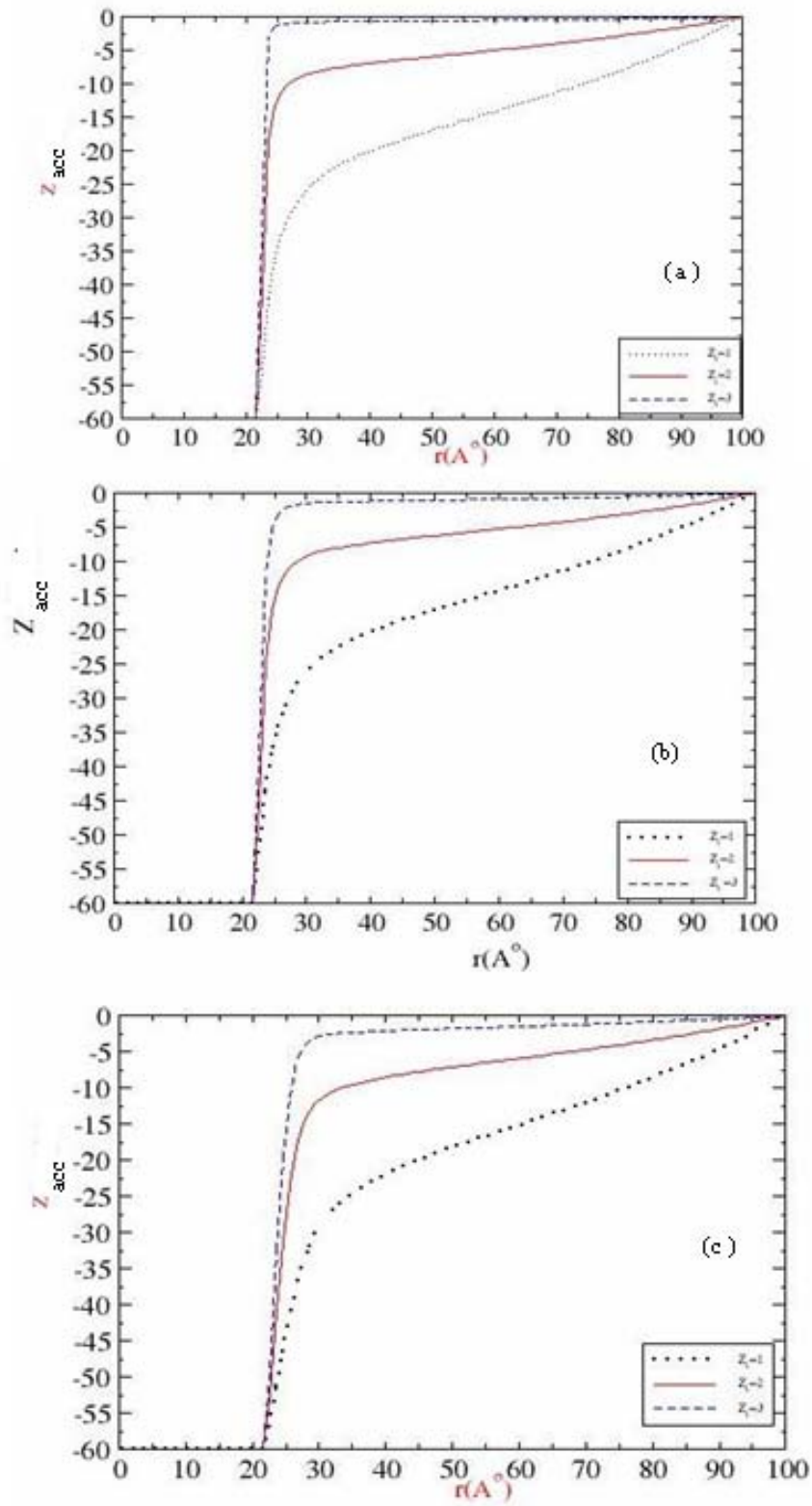


Figure3.8: Accumulated charge for the system with (a) central (b) mobile surface (c) mobile protruding charge distribution models at different valence of counterion.

Table 3.4: Values of Z_{eff} for the system with central charge distribution and discrete charge distribution at counterion valence (a) $Z_i=1$, (b) $Z_i =2$ and $Z_i=3$ at $r = 25 \text{ \AA}$

(a) $Z_i=1$

model	Z_{eff} at $r = 25 \text{ \AA}$
c	-36
ms	-35
mp	-44

(b) $Z_i=2$

model	Z_{eff} at $r = 25 \text{ \AA}$
c	-15
ms	-12
mp	-27

(c) $Z_i=3$

model	Z_{eff} at $r = 25 \text{ \AA}$
c	-4
ms	-1
mp	-15

From Z_{acc} the EDL potential has been calculated as the following equation:

$$\Psi_{\text{EDL}} = Z_{\text{acc}} / 4\pi\epsilon_0\epsilon_r r \quad \text{Eq. 7}$$

Where Ψ_{EDL} is EDL potential Z_{acc} accumulated charge.

The results are shown in figures 3.9 and 3.10 the values of surface potentials (Ψ_0) at $r = 22 \text{ \AA}$ and potentials of the diffused part of the EDL (Ψ_d) has been obtained. The values are affected by changing from uniform to discrete charge distributions and by counterions valence, this is because the accumulation of counterions is changed.

For all counterions valences the effect of discretization is seen in figure 3.9, at the surface of macroion $r = 22 \text{ \AA}$ the value of Ψ_0 in case of mobile protruding is less than others this is

because of the volume of the charge. In case of $Z_i = 1$ the accumulated charge for mobile point is = -47, for central = -49 and for mobile protruding = -54.

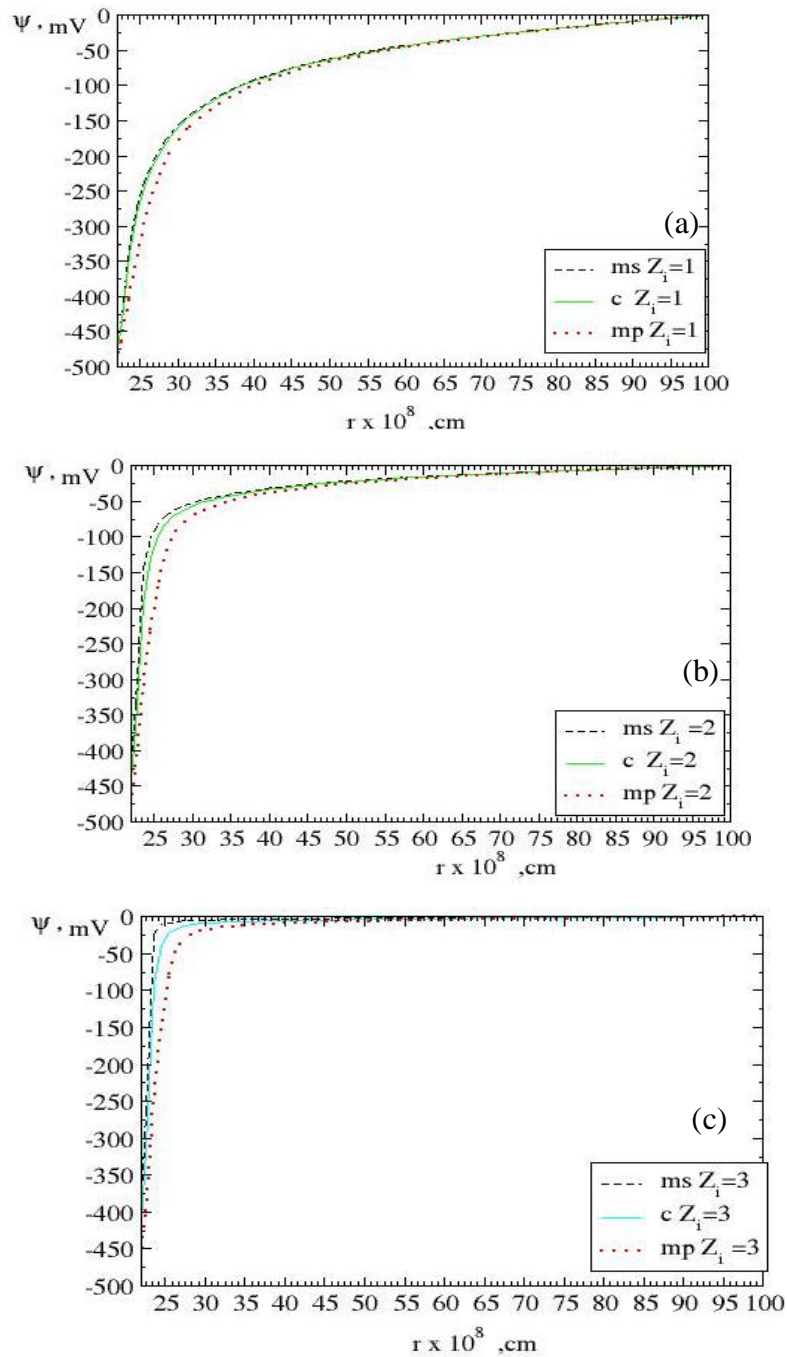


Figure 3.9: The potential at counterion valence (a) $Z_i = 1$, (b) $Z_i = 2$ and $Z_i = 3$ for central distribution model and discrete charge distribution.

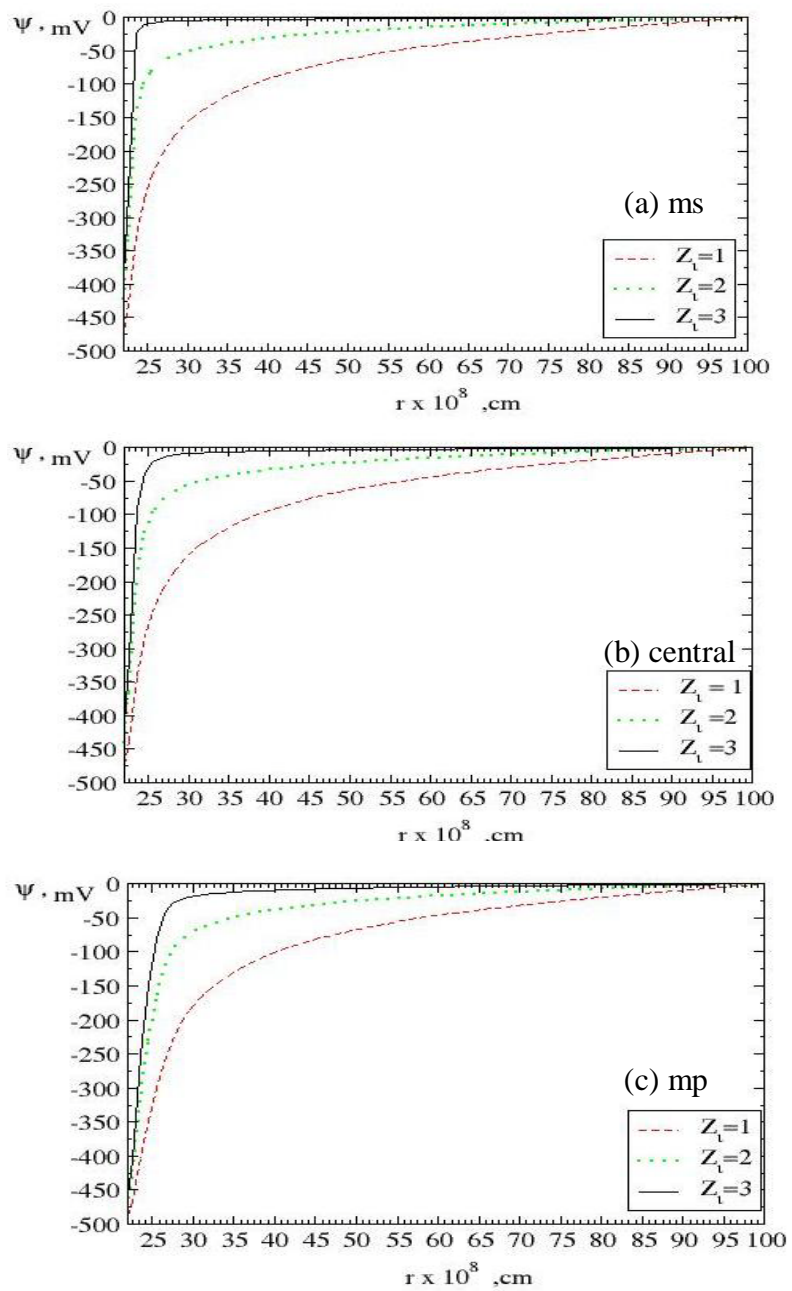


Figure 3.10 : Electrostatic potential for the systems with central and discrete charge distribution models at counterion valence $Z_i=1, 2, 3$ (a)central,(b)ms (c) mp

Table 3.5: Potential for central charge distribution model and discrete charge distribution at counterion valence (a) $Z_i = 1$ (b) $Z_i = 2$ and $Z_i = 3$ at the surface of macroion (Ψ_0 Surface potential) $r = 22 \text{ \AA}$ and (Ψ_d diffused potential) at $r = 30 \text{ \AA}$.

(a) $Z_i = 1$

model	Ψ_0	Ψ_d
c	-474	-161
ms	-470	-157
mp	-488	-180

(b) $Z_i = 2$

model	Ψ_0	Ψ_d
c	-439	-56
ms	-423	-52
mp	-472	-72

(c) $Z_i = 3$

model	Ψ_0	Ψ_d
c	-412	-9
ms	-387	-5
mp	-459	-18

The counterion-counterion radial distribution $g_{ii}(r)$ measures the relative density of particles of type i (counterion) at distance r from a particle of type also i (counterion) affected by discretization and valences. The shape of $g_{ii}(r)$ reflects the combined effect of the attraction between the counterions and the macroion, and the repulsion among the counterions themselves.

Figure 3.11 indicates that counterion-counterion radial distribution functions which display the same qualitative features independent of the valence of the counterions.

For all charge distributions models the correlation between trivalent ions is much stronger than the correlation between divalent counterions and the later is stronger than between monovalent counterions. The effect of discretization of the charges also appears, there is stronger correlations in case of mobile point surface charge compare with uniform charge distribution

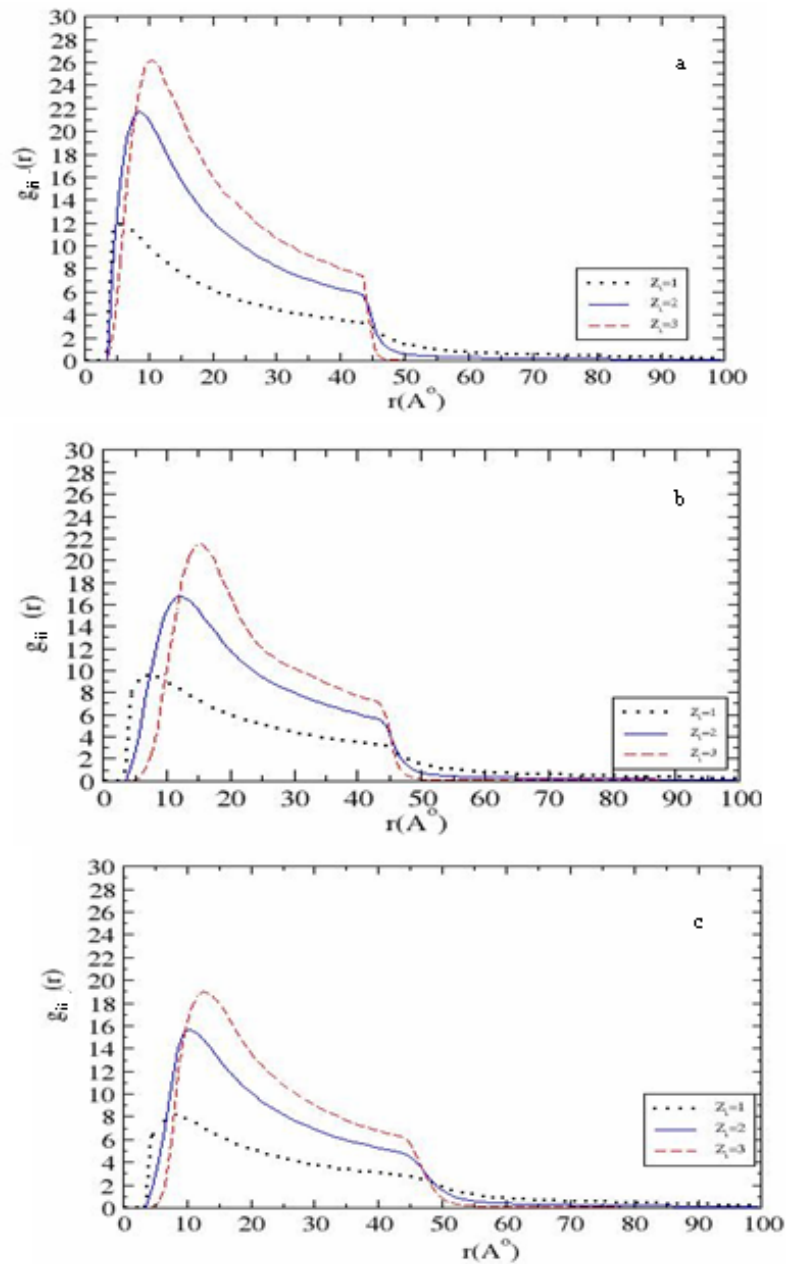


Figure 3.11: Counterion-counterion radial distribution functions for the systems at counterion valences $Z_i=1, 2, 3$ for (a) mobile surface, (b) uniform and (c) mobile protruding charge distributions

The values of maximum $g_{ii}(r)$ for all charge distributions at different counterion valences are shown in the table

Table 3.6: Maximum counterions-counterions radial distributions for all charges distributions models at counterion valence $Z_i=1, 2$ and 3 .

counterion valence	central charge distribution		Mobile surface charge distribution		Mobile protruding charge distribution	
	r in Å	Max g_{ii}	r in Å	Max g_{ii}	r in Å	Max g_{ii}
$Z_i=1$	7	9.5	6	12	8	8
$Z_i=2$	12	16.5	8.5	21.5	10	15
$Z_i=3$	15	21.5	10.5	26	13	19

3.2 Effect of adding salt

The fraction of counterions of +1valence is decreased by increasing the β value, (amount of simple 1:3 electrolyte expressed as the trivalent counterion -to-macroion charge ratio β) Where the value of β is calculated as

$$\beta = N_{ca} Z_{ca} / N_M Z_M \quad \text{Eq.8}$$

N_{ca} number of trivalent counterion Z_{ca} charge of trivalent counterion and N_M number of macroion Z_M charge of macroion.

This is because of the effect of +3 counterions and the -1 coions of salt. Ions cause inversion of the macroion charge which in turn changes the macroion counterions interaction. As the charge inversion occurred the macroion will repel counterions and more coions come closer to the macroion.

Figure 3.12 shows the counterions distribution in the vicinity of macroion (a) macroion-trivalent counterion (cation) and (b) macroion-monovalent counterion rdfs at the indicated amount of simple 1:3 electrolyte expressed as the trivalent counterion -to-macroion charge ratio β at $Z_i=1$ for the system with central charge distribution .

Figure 3.12 (b) demonstrates the accumulation of counterions near the macroion, as more salt is added the maxima decreases.

Figure (a) shows a strong accumulation of trivalent counterion near the macroion and approaches unity at large separation

The macroion-anion rdfs is quantified in figure 3.13. Anions are expelled from the vicinity of the macroion at low salt concentration as $\beta= 0.15, 0.45$ and this effect is decreased upon the addition of salt and the more anion are in the vicinity of the macroion.

The location of the maximum at $r=26 \text{ \AA}$ means that there are a layer of counterions between the macroion and the coions. This maximum is due to ion-ion correlations.

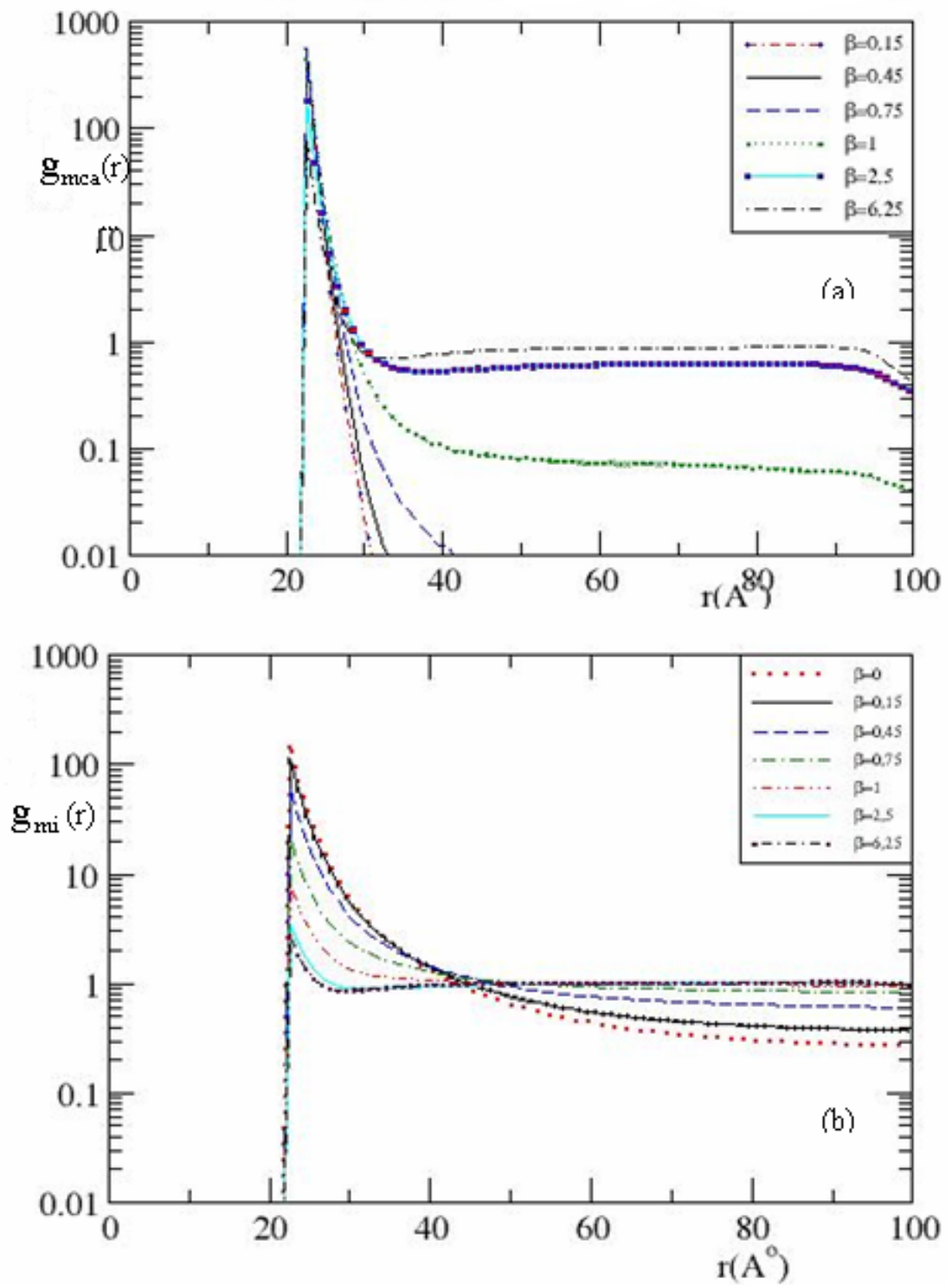


Figure 3.12: (a) Macroion-trivalent counterion (cation) and (b) macroion-monovalent counterion rdFs at the indicated amount of simple 1:3 electrolyte expressed as the trivalent Counterion -to-macroion charge ratio β at $Z_i=1$ for the system with central charge distributions.

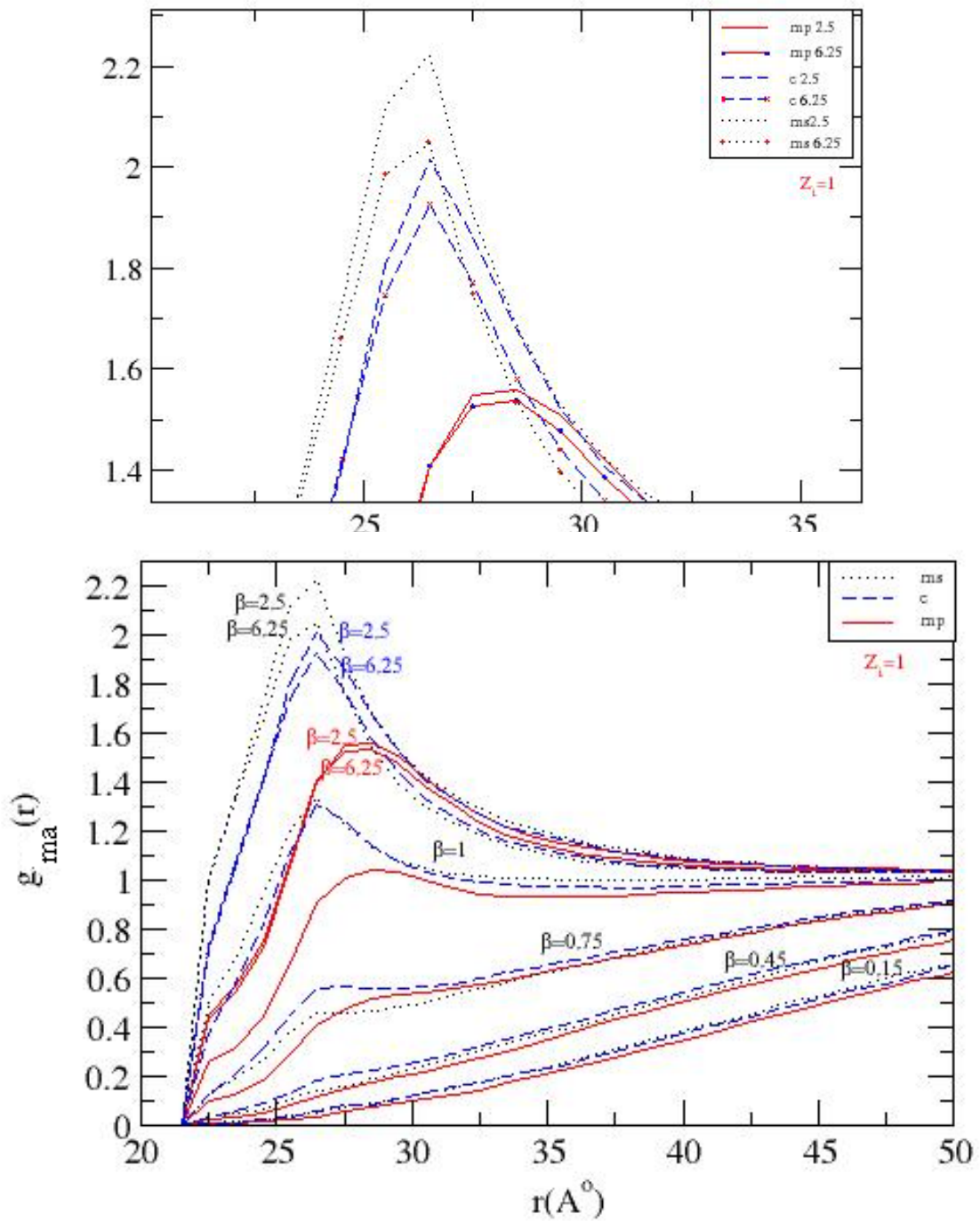


Figure 3: 13 .Macroion-coions radial distribution functions at indicated amount of simple 1:3 electrolyte expressed as the trivalent counterion -to-macroion charge ratio β at uniform and discrete Charge distributions.

For the systems with mobile protruding charge distribution at $Z_i=1$, we can see the accumulation of ions near the macroion in (a) case of salt free, the most of monovalent counterions accumulated near the macroion whereas minority is far from it, at (b) low salt concentration $\beta=0.75$ all of trivalent counterions are accumulated close to the macroion and the monovalent counterions becomes less inhomogeneously distributed but coions are found far away from macroion, at (c) $\beta=6.25$ more and several coions are very close to macroion.

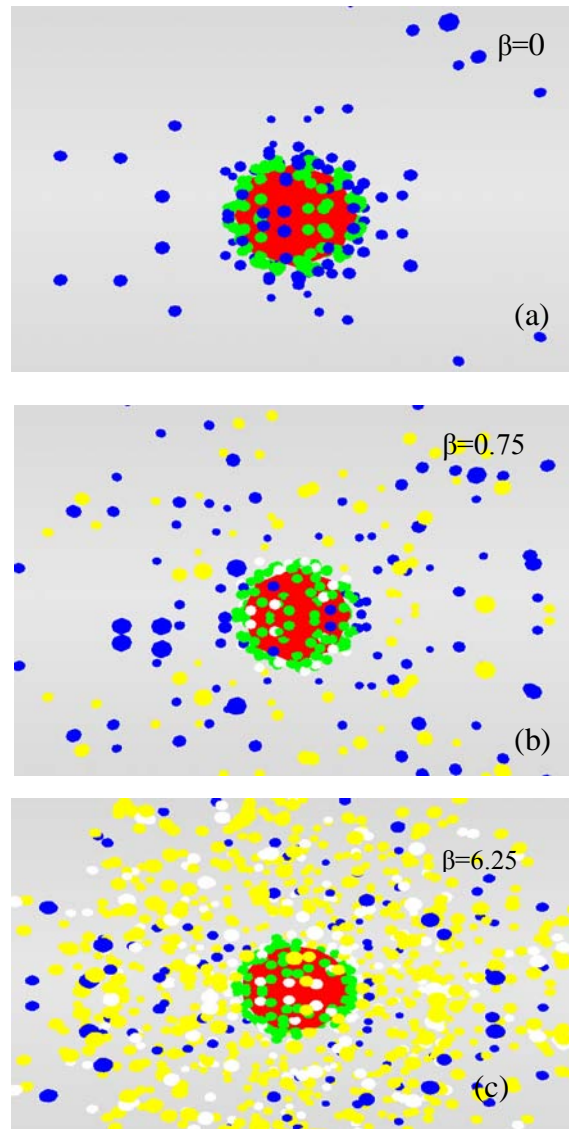


Figure 3.14 : Snapshots of systems containing one macroion (red sphere) , monovalent counterions (blue sphere) , trivalent counterions (White sphere) , coions (yellow sphere) , surface charge (Green sphere) at $Z_i=1$ in case of mobile protruding charge distributions at different amounts of the simple salt 1:3 electrolyte expressed as the trivalent counterions to macroion charge ratio (a) $\beta =0$, (b) $\beta=0.75$,and (c) $\beta=6.25$ all particles are enclosed in spherical cell.

The counterion-counterion radial distribution functions at counterions valence $Z_i = 1$ from central charge distribution in the presence of salt at different concentrations, after the addition of 1:3 salt the value of the maximum of counterion-counterion radial distribution (g_{ii}) is decreased by increasing β .

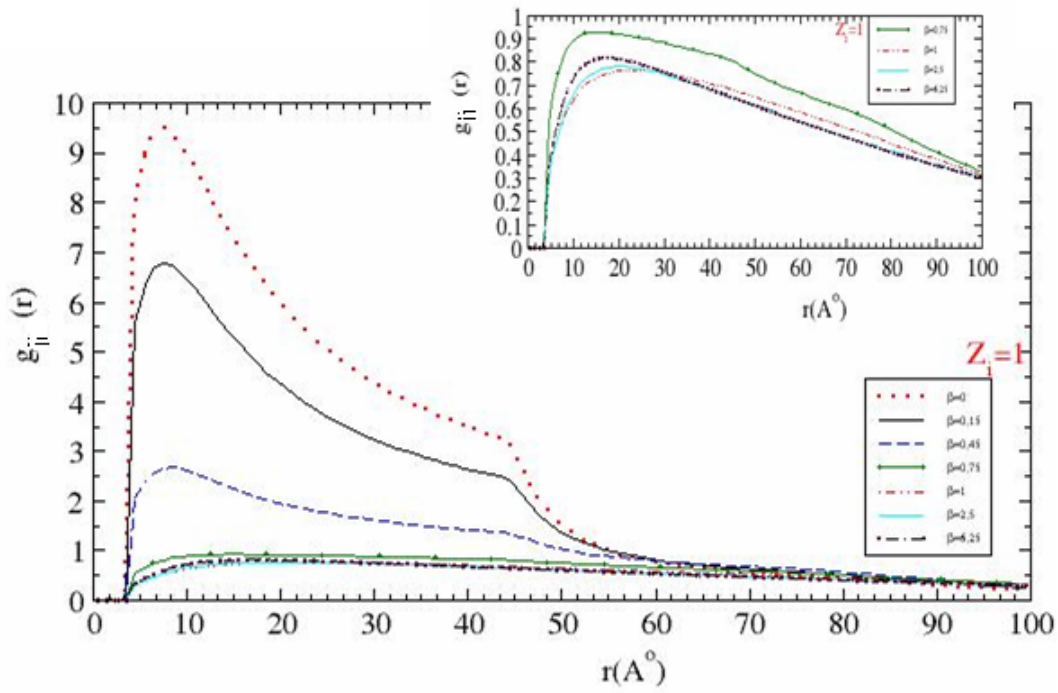


Figure 3.15: Counterion-counterion radial distribution functions at counterions valence $Z_i=1$ with central charge distribution in the presence of salt at different concentration.

Table 3.7: Maximum counterions-counterions rdfs for the system of central charges distributions at counterion valence $Z_i=1$ at $\beta=0, 0.15,$ and 0.45 .

Value of β	Separation in \AA	Value of maximum g_{ii}
0	7.5	9.5
0.15	7.5	6.7
0.45	8.5	2.6

The counterion-counterion radial distribution functions at counterions valence $Z_i = 1$ from mobile protruding charge distribution in the presence of salt at different concentrations, after the addition of 1:3 salt the value of the maximum of counterion-counterion radial distribution (g_{ii}) is decreased by increasing β .

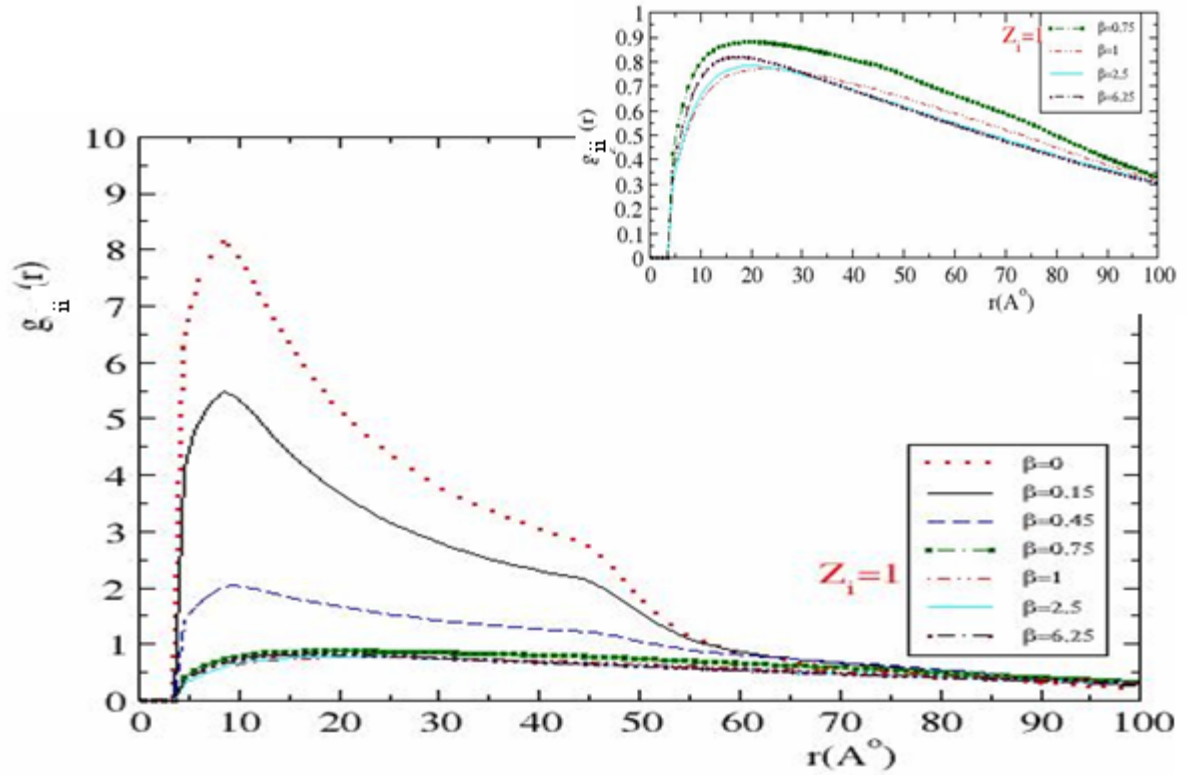


Figure 3.16: Counterion-counterion radial distribution functions at counterions valence $Z_i=1$ with protruding charge distribution in the presence of salt at different concentration

Table 3.8: Maximum counterions-counterions rdfs for mobile protruding charges distributions model at counterion valence $Z_i=1$ at $\beta = 0, 0.15,$ and 0.45 .

Value of β	$(r) \text{ \AA}$	Maximum g_{ii}
0	8	8
0.15	8.5	5.5
0.45	9.5	2.5

The counterion-counterion radial distribution functions at counterions valence =1 from surface charge distribution in the presence of salt at different concentrations, after the addition of 1:3 salt the value of the maximum of counterion-counterion radial distribution (g_{ii}) is decreased by increasing the value of β .

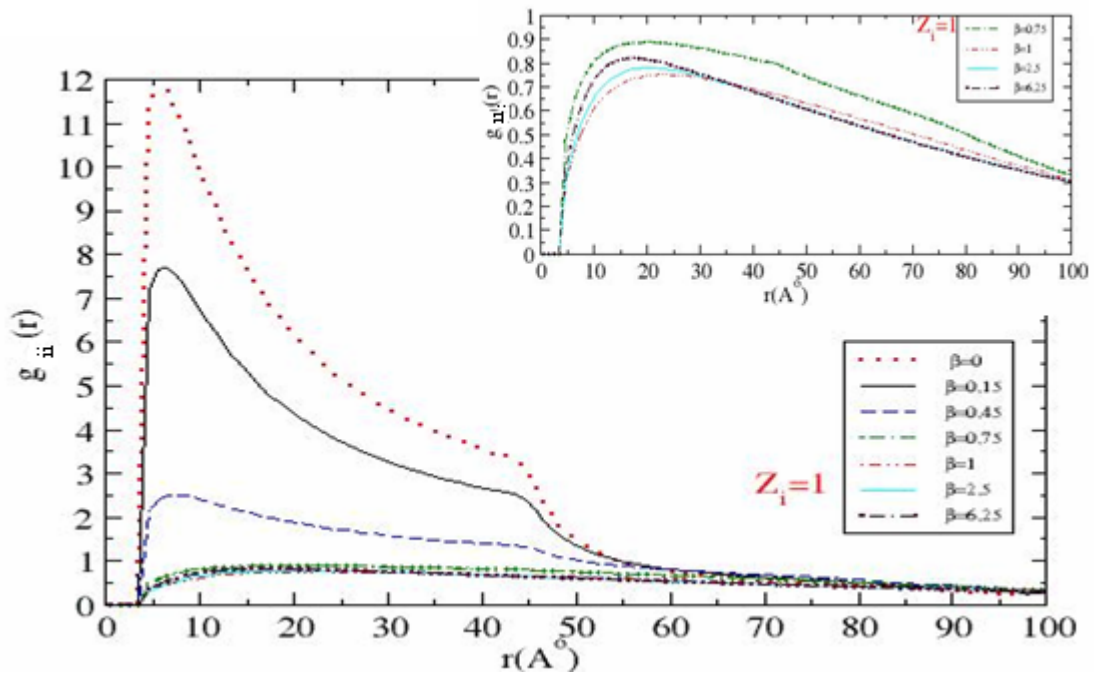


Figure 3.17. Counterion-counterion Radial distribution functions at counterions valence $Z_i=1$ with mobile surface charge distribution in the presence of salt at different concentration

Table 3.9: Maximum counterions-counterions rdfs for mobile surface charges distributions model at counterion valence $Z_i=1,2$ and 3 at $\beta = 0, 0.15,$ and 0.45 .

Value of β	(r) \AA	maximum g_{ii}
0	6	12
0.15	6	8
0.45	6.5	2.5

The effect of adding salt on the accumulated charge of the macroion is shown in figure 3.18 in case of central and discrete charge distributions models. In all models the accumulated charge increases as increases the salt concentration.

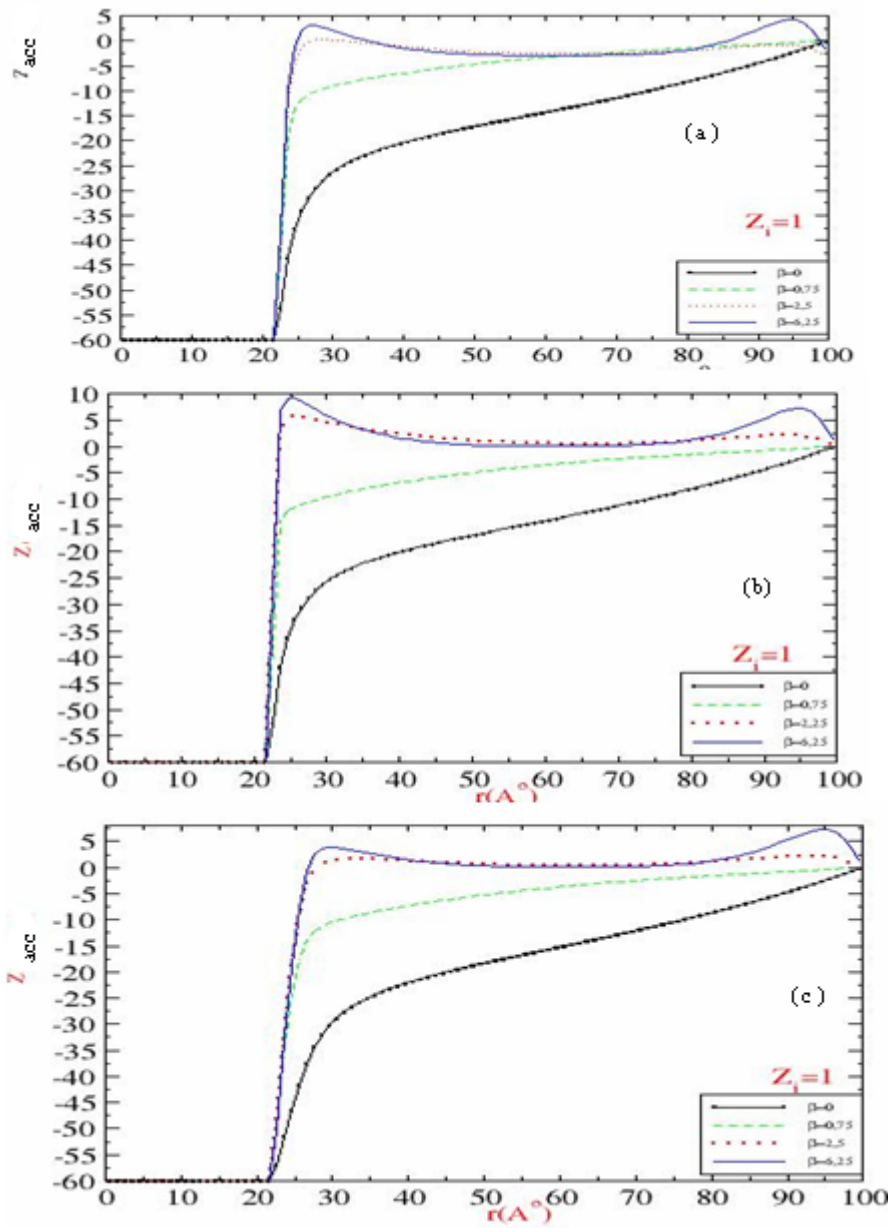


Figure 3.18: Accumulated charge for (a) central and (b) mobile surface (c) mobile protruding charge distribution at different values of β

The Z_{acc} of the macroion seen in table 3.10 are taken from graph 3.18, salt cause inversion in the macroion charge.

Table 3.10: Effective charge for the system with central and discrete charge distributions at $\beta = 0, 0.75, 2.5, 6.25$.

(a) central

β	$Z_{eff} \ r = 25 \text{ \AA}$
0	-36
0.75	-12
2.5	-3
6.25	+1

(b) mobile surface

β	$Z_{eff} \ r = 25 \text{ \AA}$
0	-35
0.75	-12
2.5	+6
6.25	+9

(c) mobile protruding

β	$Z_{eff} \ r = 25 \text{ \AA}$
0	-44
0.75	-21
2.5	-14
6.25	-13

As seen in figure 3.19 the potential is increased by adding salt, the figure shows the potential at $\beta=0$ salt free system and at $\beta 0.75$. The effect of adding salt on potential is shown in figure 3.20 for case of central and discrete charge distributions models.

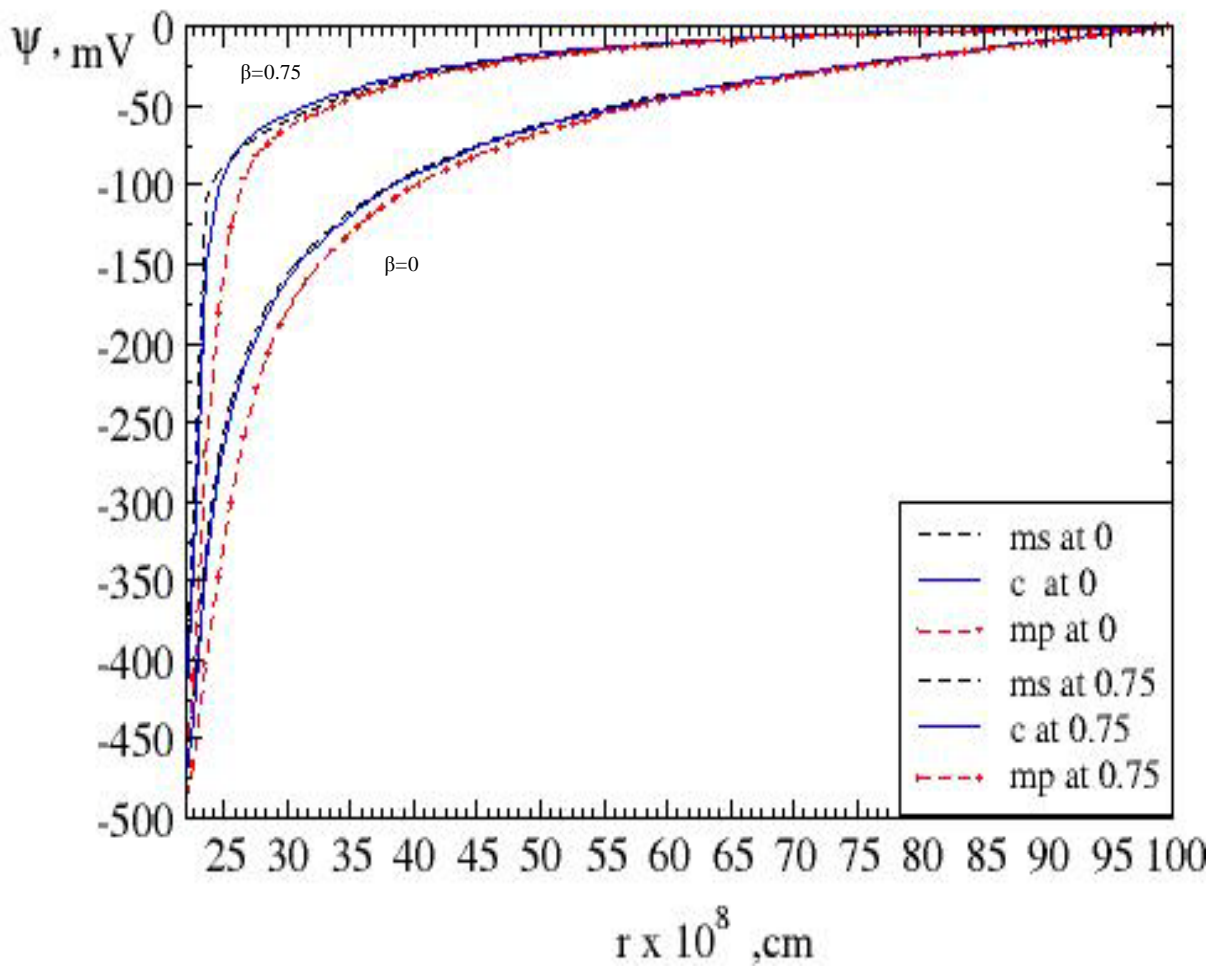


Figure 3.19 .The potential for the systems of central and discrete charge distributions at counterion valences $Z_i=1$ at $\beta=0$, and 0.75

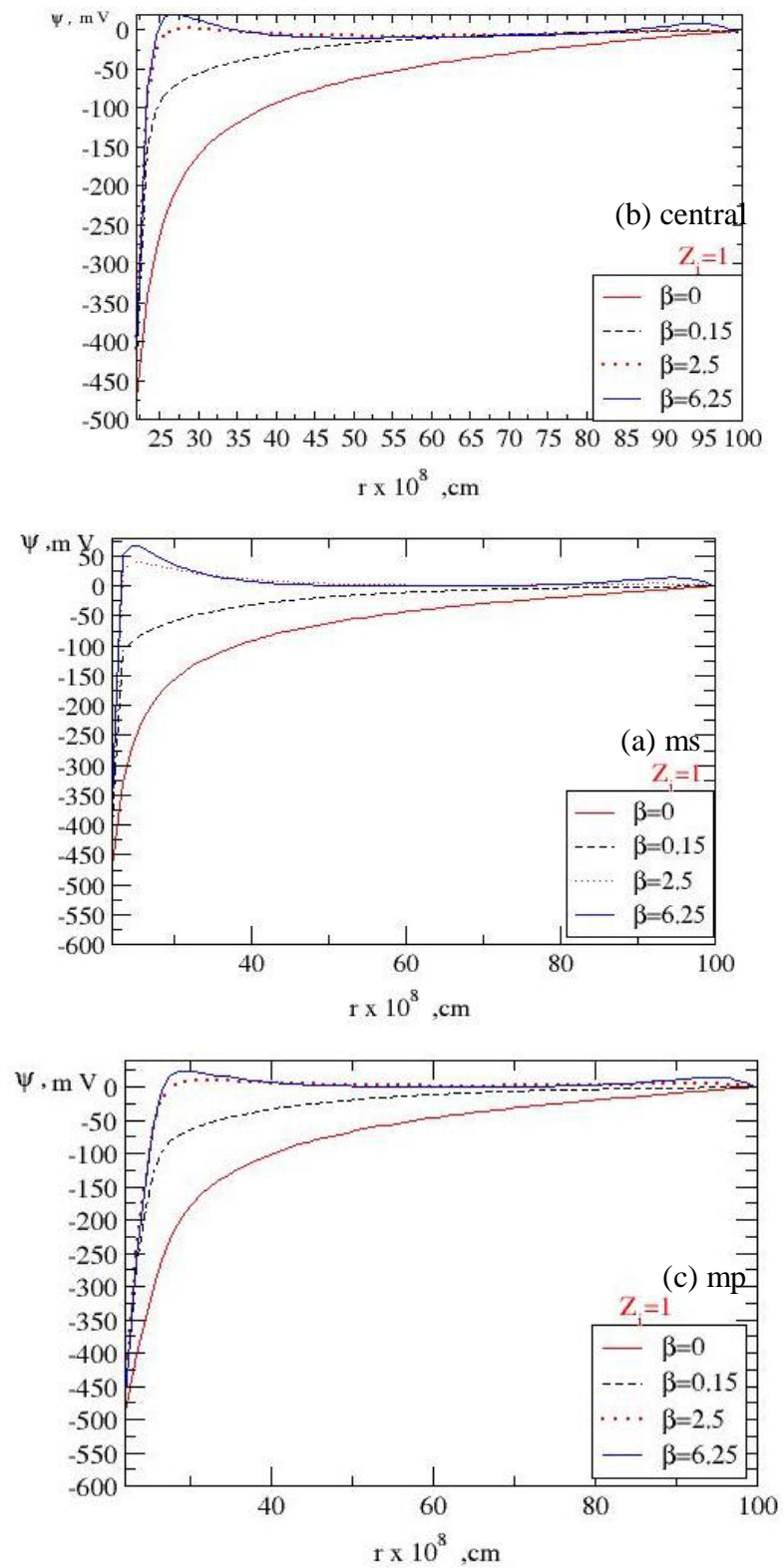


Figure 3.20: Electrostatic potential for the system with central and discrete charge distributions at counterion valence of $Z_i=1$ at different concentrations of salt.

Table 3.11: Electrostatic potential for the system with central and discrete charge distributions at counterion valence of $Z_i=1$ at different concentrations of salt.

(a) central

β	Ψ_s	Ψ_d
0	-474	-161
0.75	-424	-56
2.5	-413	+1
6.25	-411	+14

(c) mobile surface

β	Ψ_s	Ψ_d
0	-470	-157
0.75	-407	-57
2.5	-375	+27
6.25	-368	+37

(b) mobile protruding

β	Ψ_s	Ψ_d
0	-488	-180
0.75	-460	-65
2.5	-460	+10
6.25	-461	+22

3.3 Effect of the size of counterions

Figure 3.21 shows the charge density $\rho(r)$ of counterions, of different sizes, in the vicinity of macroion. As we can see the density is affected by the volume of the counterions, it is decreased by increasing the volume of the counterions with all distribution models and all valences.

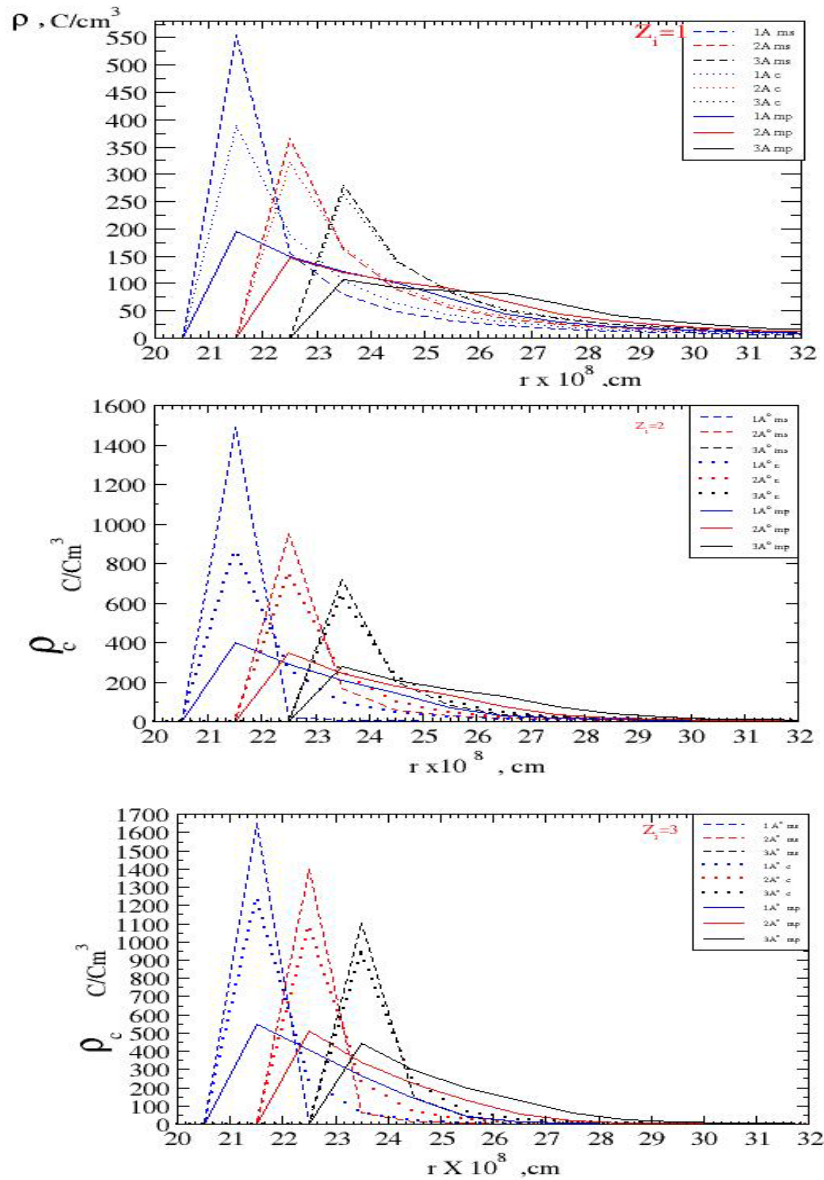


Figure 3.21: Local charge density at $Z_i=1, 2, 3$ for the system with discrete and central charge distributions at different radii of counterions.

Figure 3.22 shows the accumulated charge (Z_{acc}) of the macroion for the systems with different sizes of counterions.

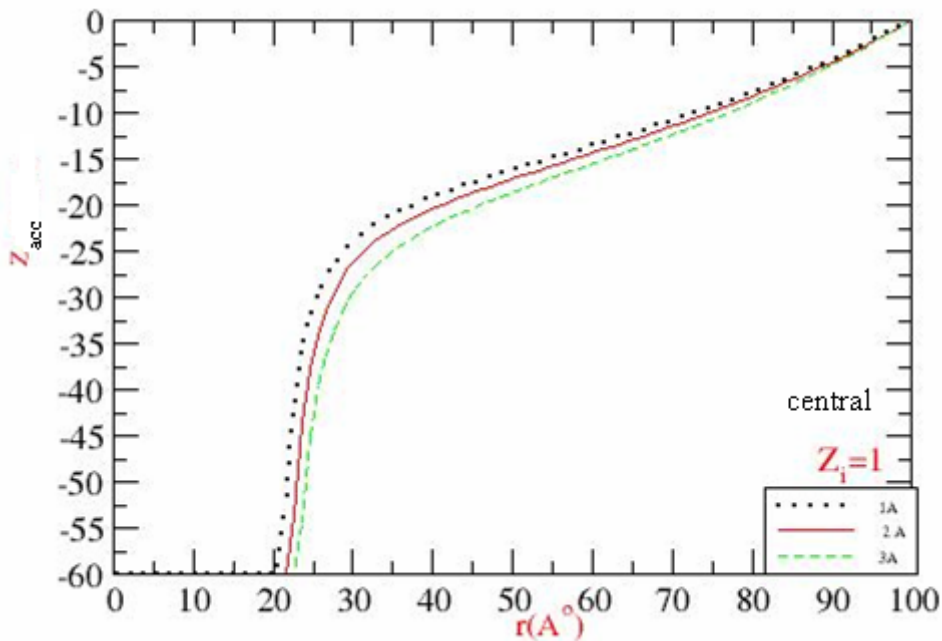


Figure 3.22: Accumulated charge for central charge distribution at different radii of counterion.

Table 3.12 shows the effective charge of macroion with different sizes which is larger with larger size.

Table 3.12: Effective charge for the system with central charge distribution at $Z_i = +1$ with counterion radius = 1, 2 and 3 at 25 Å

counterions radius	(Z_{eff} at $r=25$) Å
1 Å	-31
2 Å	-35
3 Å	-42

Potential in the EDL change by changing the radius of counterions .Figure 3.23 shows the potential for uniform and discrete charge distributions at different counterions radii(1,2and 3 Å) at 22 Å and at 30 Å . The potential is decreased by increasing the radius and approach zero at large separation from the macroion.

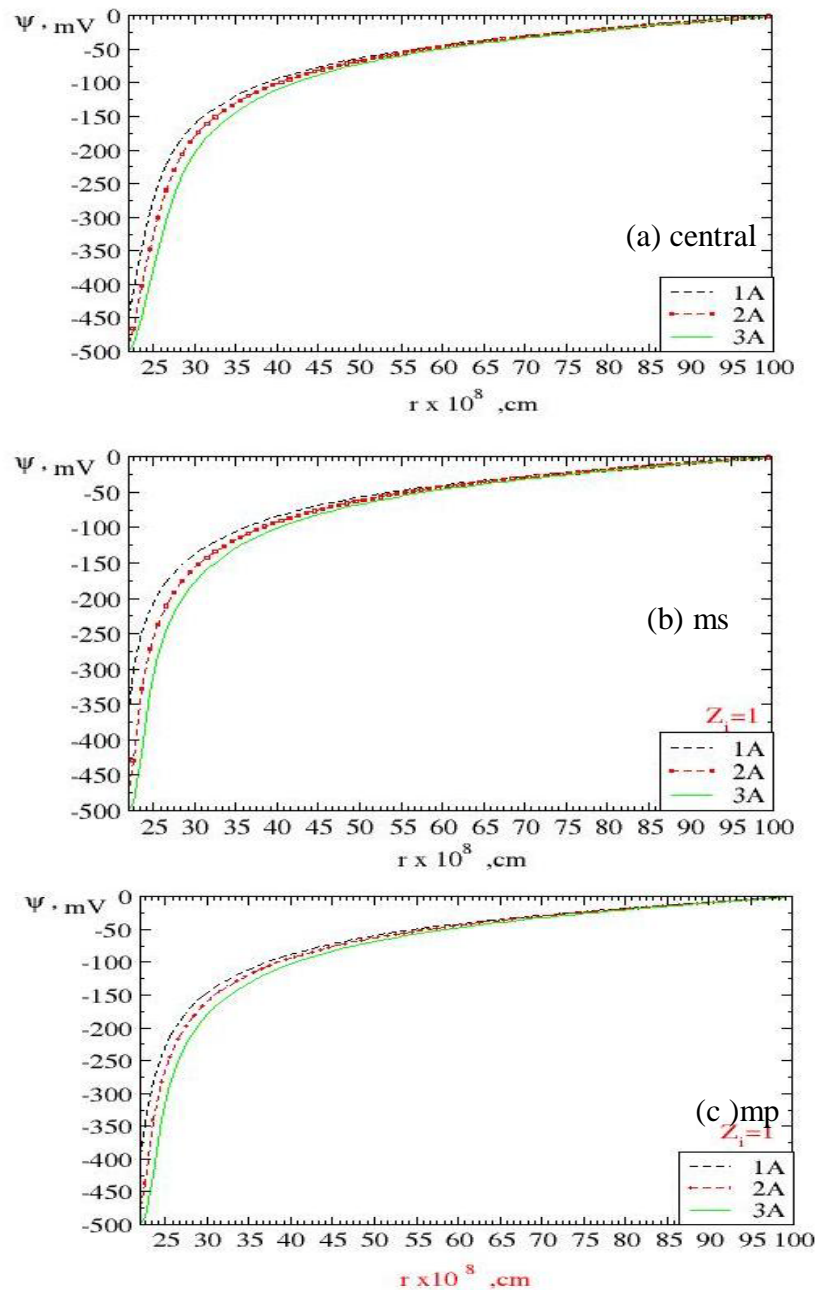


Figure 3.23: The electrostatic potential for the system with (a) uniform (central) (b) mobile surface (ms) and (c) mobile protruding (mp) charge distributions at different counterions radii (1,2and 3 Å).

In table 3.13 we see that Potential decreases by increasing the counterions volume, these values has been taken from figure 3.23

Table 3.13: Potential for Potential charge distribution model and discrete charge distribution at counterion radius 1 Å, 2 Å, and 3 Å.

radius	central charge distribution		Mobile surface charge distribution		Mobile protruding charge distribution	
	Ψ_s	Ψ_d	Ψ_s	Ψ_d	Ψ_s	Ψ_d
1 Å	-495	-147	-481	-138	-506	-162
2 Å	-474	-161	-470	-157	-488	-180
3 Å	-455	-181	-453	-178	-468	-205

Chapter Four

conclusion

Conclusions

Monte Carlo simulations have been carried out to elucidate the structure of the electric double layer (EDL) in contact with discrete and continuously charged sphere macroion surfaces.

The performed simulation was based on a primitive model of electrolyte solutions used in the framework of Mc-Millan–Mayer theory. The solvent is treated as a dielectric medium solely characterized by its relative permittivity ϵ_r equal to that of bulk water at T 298K. Whereas the colloids (later referred to as macroions), the counterions, cations and anions are represented by charged hard spheres.

It was carried in the canonical ensemble, at constant number of particles, volume, and temperature according to the standard Metropolis algorithm. The configurations were generated by first placing the macroion in the center of the spherical cell. The macroion charges were positioned according to the different charge distributions. Finally, the counterions were positioned randomly. $2 \cdot 10^6$ attempted MC moves per particles were made in the production runs. All the simulations were performed using the integrated Monte Carlo/molecular dynamics/ Brownian dynamics simulation package MOLSIM.

Mobile charge discretization models (point charges localized on the macroion surface and finite-sized charges protruding into the solution) are considered together with the case of uniform charge distribution (central). The distribution of counterions near a macroion was determined using a spherical cell. The effect of discreteness, radius of the counterions and the presence of salt was analyzed in terms of radial distribution functions, charge density profiles, accumulated charge and potential profiles.

It was established that with protruding charges the counterions are less accumulated near the macroion because the excluded volume effect dominating over the increased correlation ability. But with point charges distributions, counterions become more strongly accumulated to the macroion and the effect increases with counterion valence.

The macroion-counterion electrostatic increases in magnitude when the counterion valence increases leading to a more uneven counterion distribution. As we saw the correlation between trivalent ions and macroion is much stronger than the correlation in case of divalent counterions which is stronger than correlation between monovalent ions and macroion. The effect of changing the surface charge distribution from the central to mobile distribution becomes more pronounced as the counterion valence is increased. For all counterion valences the g_{mi} in mobile surface charge distribution system are larger than in central one which are more than mobile protruding charge distribution. And as increasing the valences the g_{mi} increases for all charge distribution system.

The counterion-counterion radial distribution $g_{ii}(r)$ measures the relative density of particles of type i (counterion) at distance r from a particle of type also i (counterion) affected by discretization and valences. The shape of $g_{ii}(r)$ reflects the combined effect of the attraction between the counterions and the macroion, and the repulsion among the counterions themselves. For all charge distributions models the correlation between trivalent ions is much stronger than the correlation between divalent counterions and the later is stronger than between malevolent counterions. There are stronger correlations in case of mobile point surface charge compare with uniform charge

Ions cause inversion of the macroion charge which in turn changes the macroion counterions interaction. As the charge inversion occurred the macroion will repel counterions and more coions come closer to the macroion

Local charge density, was calculated from rdfs, which means how many charges in the volume at the vicinity of the macroion. Its value increases and its dispersion decreases by increasing the valence and its value in mobile surface charge distribution is more than in case of central charge distribution. The values are affected by changing from uniform to discrete charge distributions and by counterions valence, this is because the accumulation of counterions is changed.

At low salt concentration anions are expelled from the vicinity of the macroion and this effect is decreased upon the addition of salt and the more anion are in the vicinity of the macroion.

After the addition of 1:3 salt the value of the maximum of counterion-counterion radial distribution (g_{ii}) is decreased by increasing β . In all models the accumulated charge increases as increases the salt concentration.

The local charge density is affected by the volume of the counterions, it is decreased by increasing the volume of the counterions with all distribution models and all valences.

Potential in the EDL change by changing the radius of counterions. The potential is decreased by increasing the radius and approach zero at large separation from the macroion.

At low salt concentration, the macroion accumulated charge is reduced due to multivalent counterion adsorption. At high salt concentrations, the macroions become overcharged so that their apparent charge has the opposite sign to the stoichiometric one. The character of charge distribution affects the EDL structure near the macroion, whereas its effect is much weaker at larger distances.

Valences of counterion play an important role in the structure of EDL, in all models the counterion layer near the macroion becomes more compact with an increase in charge multiplicity. As the valences of counterion increased, screening of macroion charge is increased that leads, correspondingly, to decrease in the absolute value of the surface potential of macroion. The salt affects the ionic distributions in the EDL and also the potential, at low salt concentration the trivalent counterions come close to the macroion and the coions are expelled out, as the salt increases the coions exhibit tendency to the concentration in the macroion ionic atmosphere, then this will change the macroion accumulated charge and the EDL potential. Future works will address the distribution of counterions in the electric double layer at finite temperature, at present of other salt type and concentrations.

References

- ¹ - (Rojj 2010) Roij R. V., (2010): (Electrostatics in liquids: From electrolytes and suspensions towards emulsions and patchy surfaces)," *Physica A: Statistical Mechanics and its Applications*" Article in Press.
- ² (Shaw 1992) Shaw D. J., (1992): Introduction to Colloid and Surface Chemistry (4th Ed), Elsevier Science Ltd.
- ³ - (Debye and Huckel 1923) Debye P., and Huckel E., (1923): (The theory of electrolytes. I. Lowering of freezing point and related phenomena)," *Physikalische Zeitschrift*", Vol. 24, PP. 185-206.
- ⁴ - (Bjerrum 1926) Bjerrum N.(1926): (Analysis of ionic association)" *Kgl. Dan. Vidensk. Selsk. Mat.-Fys. Medd*",Vol.7:9, PP.1-48.
- ⁵ - (Deryaguin and Landau 1941) Deryaguin B. and Landau . D, (1941) : (A theory of the stability of strongly charged lyophobic sols and of the adhesion of strongly charged particles in solutions of electrolytes). "*Acta Physicochim. USSR*", Vol. 14, PP. 633-652.
- ⁶ - (Verwey and Overbeek 1948) Verwey E. W. and Overbeek J. T. G., (1948): (theory of Stability of Lyophobic Colloids) Elsevier, Amsterdam.The Netherlands.
- ⁷ - (Ravindran and Wu 2005) Ravindran S. and Wu J., (2005):(Ion size effect on colloidal forces within the primitive model)" *Condensed Matter Physics*", Vol. 8: 2(42), PP. 377-388.
- ⁸ - (Sogami and Ise 1984) Sogami I.,and Ise N., (1984): (On the electrostatic interaction in macroionic solutions)" *J. Chem. Phys*", Vol. 81:6, PP. 6320-6332.
- ⁹ - (Kjellander et.al. 1990) Kjellander R., Marcelja S., Pashley R. M., and Quirke J. P., (1990): (A theoretical and experimental study of forces between charged mica surfaces in aqueous CaCl₂ solutions)" *Chem. Phys.* ", Vol. 92:7, PP. 4399-4407.
- ¹⁰ - (Guldbrand et.al. 1984) Guldbrand L., Jönsson B., Wennerström H., and Linse P., (1984) :(Electric double layer forces .A Monte Carlo study)" *J. Chem. Phys.*",Vol. 80, PP.2221-2228.
- ¹¹ - (Kjellander and Marcelja 1984) Kjellander R. and Marcelja S. (1984): (Correlation and image charge effect in electric double layers) "*Chem. Phys. Lett.*", Vol.112 :1, PP.49-53.
- ¹² - (Belloni 2002) Belloni L., (2002) (Colloid-counterion mixtures: an advanced integral equation) "*J.Phys.: Condens. Matter.*", ,Vol. 14:40, PP.9323.
- ¹³ - (Lobaskin and Qamhieh2003) Qamhieh K. and Lobaskin V., (2003): (Effective Macroion Charge and Stability of Highly Asymmetric Electrolytes at Various Salt Conditions)" *J. Phys. Chem. B* ", Vol.107, PP.8022 -8028.

-
- ¹⁴ - (Qamhieh and Linse 2005) Qamhieh K. and Linse P. , (2005) : (Effect of discrete macroion charge distributions in solutions of like-charged macroions) " J. CHEM. PHYS." Vol. 123, PP.104901.
- ¹⁵ - (Naji and Netz 2004) Naji A. and Netz R. R., (2004): (Attraction of like-charged macroions in the strong-coupling limit) " The European Physical Journal E: Soft Matter and Biological Physics", Vol.13:1, PP.43-59.
- ¹⁶ - (Vlachy 1999)Vlachy V. (1999): (Ionic effects beyond Poisson Boltzmann theory) " Annu. Rev. Phys. Chem." Vol. 50, PP.145–65.
- ¹⁷ - (Bhuiyan 2002) Bhuiyan B., Vlachy V. and Outhwaite C. W.,(2002) : (Understanding polyelectrolyte solutions: macroion condensation with emphasis on the presence of neutral co-solutes) " Int. Reviews in Physical Chemistry' ,Vol. 21: 1, PP.1-36.
- ¹⁸ -(Belloni 2000) Belloni L.,(2000):(Colloidal interactions)," J. Phys.Condens. Matter"Vol. 12, PP. R549-R587.
- ¹⁹ - (Hansen and Löwen, 2000) Hansen J.-P. and Löwen H,(2000): (Effective interactions between electric double layers) " Annu. Rev. Phys. Chem.", Vol.51:1, PP.209-242.
- ²⁰ - (Messina et.al. 2002) Messina R., Holm C., and Kremer K., (2002) : (Charge inversion in colloidal systems) " Computer Physics Communications" ,Vol. 147, PP. 282-285 .
- ²¹ - (Messina et.al.(july)-2001) Messina R., Holm C., and Kremer K., (2001)(Strong electrostatic interactions in spherical colloidal systems) " Phys. Rev.E" ,Vol.64:2, PP.021405.
- ²² - (Semashko et.al. 2005) Semashko O. V., Brodskaya E. N., and Us'yarov O. G., (2005): (Molecular Dynamics Simulation of the Electrical Double Layer of Spherical Macroion) " J. Colloid" Vol. 67,PP. 625-630.
- ²³ - (Semashko and Brodskaya 2006) Semashko O. V. and Brodskaya E. N., (2006): (Simulation of the Electrical Double Layer of a Macroion with Different Counterion Charges) " J. Colloid ", Vol.68:5, PP.617-622.
- ²⁴ - (Molina et.al.2006) Molina A. M., Perez M. Q., and Alvarez R. H., (2006):(Electric Double Layers with Electrolyte Mixtures: Integral Equations Theories and Simulations) " J. Phys. Chem. B", Vol.110:3,PP. 1326-1331.
- ²⁵ - (Madurga et.al. 2007) Madurga S. , Molina A. M., Vilaseca E., Mas F. , and Pérez M. Q. (2007) : (Effect of the surface charge discretization on electric double layers:A Monte Carlo simulation study) " J. Phys. Chem", Vol. 126, PP. 234703-234714
- ²⁶ - (Messina et.al. (March)-2001) Messina R., Holm C., Kremer K., (2001): (Effect of colloidal charge discretization in the primitive model) " Eur. Phys. J. ", Vol. 4, PP 363-370
- .

²⁷ - (Besteman et.al. 2008) Besteman K., Zevenbergen M. A. G., Heering H. A., and Lemay S. G. (2008) : (Direct observation of charge inversion by multivalent ions as a universal electrostatic phenomenon) "*Physical Review Letters*", VOL. 93:17, PP. 170802.

²⁸ - (Sennato et.al. 2009) Sennato S., Truzzolillo D. , Bordi F. , Sciortino F., and Cametti C. (2009): (Colloidal particle aggregates induced by particle surface charge heterogeneity) "*Colloids and Surfaces A: Physicochem. Eng.* ",Vol. 343", PP. 34-42.

²⁹ - (Holmberg 2002) Holmberg K.,(2002) : (hand book of applied surface and colloid chemistry) John Wiley & Sons Ltd

³⁰ - (Allen and Tildesley 2001) Allen M. P. and Tildesley D. J. (2001): (Computer simulation) J.W. Arrowsmith Ltd. Bristol.

³¹ - (Linse 2004) Linse P., MOLSIM , (2004)Version 4.0.0,Lund University, Lund, Sweden,

تأثير توزيع الشحنات السطحية المتميزة (الشحنات المتحركة) على طبقة مزدوجة كهربائية

أعداد: ميرفت العملة

إشراف: دخوله قمحية

الملخص:

استعملت محاكاة مونتني كارلو لدراسة هيكل طبقة مزدوجة كهربائية الموجودة حول ماكرو أيون في كل من التوزيعات الشحنية المتجانسة على السطح والتوزيعات المتميزة (discrete)

تم الأخذ بالاعتبار نظامين من أشكال التوزيع الشحني السطحي (discrete):

1. اعتبار الشحنات أنها نقطية (أي لا حجم لها) و متحركة على سطح ماكرو أيون
2. اعتبار الشحنات بارزة (لها حجم في المحلول) و متحركة على سطح ماكرو أيون

ثم مقارنة النظامين مع نظام التوزيع الشحني المتجانس (التي تكون موزعة بنظام على السطح بحيث يتم اعتبارها وكأنها في المركز).

استخدم خلية كرويه لدراسة توزيع الكونتر أيون حول الماكرو أيون ومن ثم تحليل تأثير (تمايز الشحنات السطحية) على شكل دالة توزيع شعاعي الكثافة الشحنية والجهد الكهربائي.

ثم تم تحليل تأثير حجم counter ions ووجود الملح على الكثافة الشحنية والجهد الكهربائي

ومن خلال النتائج التي تم الحصول عليها وجد انه في نظام الشحنات المتحركة البارزة في المحلول كان هنالك تجمع أقل لل counter ions وبالمقابل فانه في حال الشحنات المتحركة النقطية يصبح هنالك تجمع لل counter ions بشكل اكبر وهذا التأثير يزداد بازدياد التكافؤ الكيميائي للكونتر أيون.

وجد انه في وجود تركيز ملحي قليل فان الكثافة الشحنية لل macro ions قلت اما في التراكيز الملحية العاليه فان macro ions يصبح مزدحم بالشحنات ويحدث تغير في نوع الشحنة (charge inversion).

macro ions بالقرب من EDL وبالمحصلة النهائية فان صفات توزيع الشحنات يؤثر على تركيب وهذا التأثير يقل على المسافات البعيدة